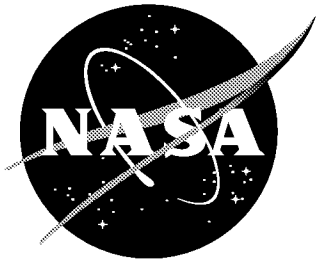


NASA/CR-2001-210874



A Small Aircraft Transportation System (SATS) Demand Model

*Dou Long, David Lee, Jesse Johnson, and Peter Kostiuk
Logistics Management Institute, McLean, Virginia*

June 2001

The NASA STI Program Office ... in Profile

Since its founding, NASA has been dedicated to the advancement of aeronautics and space science. The NASA Scientific and Technical Information (STI) Program Office plays a key part in helping NASA maintain this important role.

The NASA STI Program Office is operated by Langley Research Center, the lead center for NASA's scientific and technical information. The NASA STI Program Office provides access to the NASA STI Database, the largest collection of aeronautical and space science STI in the world. The Program Office is also NASA's institutional mechanism for disseminating the results of its research and development activities. These results are published by NASA in the NASA STI Report Series, which includes the following report types:

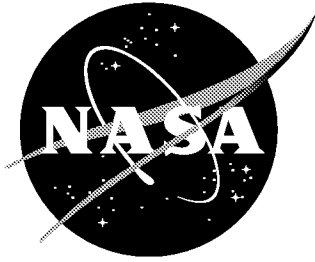
- TECHNICAL PUBLICATION. Reports of completed research or a major significant phase of research that present the results of NASA programs and include extensive data or theoretical analysis. Includes compilations of significant scientific and technical data and information deemed to be of continuing reference value. NASA counterpart of peer-reviewed formal professional papers, but having less stringent limitations on manuscript length and extent of graphic presentations.
- TECHNICAL MEMORANDUM. Scientific and technical findings that are preliminary or of specialized interest, e.g., quick release reports, working papers, and bibliographies that contain minimal annotation. Does not contain extensive analysis.
- CONTRACTOR REPORT. Scientific and technical findings by NASA-sponsored contractors and grantees.
- CONFERENCE PUBLICATION. Collected papers from scientific and technical conferences, symposia, seminars, or other meetings sponsored or co-sponsored by NASA.
- SPECIAL PUBLICATION. Scientific, technical, or historical information from NASA programs, projects, and missions, often concerned with subjects having substantial public interest.
- TECHNICAL TRANSLATION. English-language translations of foreign scientific and technical material pertinent to NASA's mission.

Specialized services that complement the STI Program Office's diverse offerings include creating custom thesauri, building customized databases, organizing and publishing research results ... even providing videos.

For more information about the NASA STI Program Office, see the following:

- Access the NASA STI Program Home Page at <http://www.sti.nasa.gov>
- E-mail your question via the Internet to help@sti.nasa.gov
- Fax your question to the NASA STI Help Desk at (301) 621-0134
- Phone the NASA STI Help Desk at (301) 621-0390
- Write to:
NASA STI Help Desk
NASA Center for AeroSpace Information
7121 Standard Drive
Hanover, MD 21076-1320

NASA/CR-2001-210874



A Small Aircraft Transportation System (SATS) Demand Model

*Dou Long, David Lee, Jesse Johnson, and Peter Kostiuk
Logistics Management Institute, McLean, Virginia*

National Aeronautics and
Space Administration

Langley Research Center
Hampton, Virginia 23681-2199

Prepared for Langley Research Center
under Contract NAS2-14361

June 2001

Available from:

NASA Center for AeroSpace Information (CASI)
7121 Standard Drive
Hanover, MD 21076-1320
(301) 621-0390

National Technical Information Service (NTIS)
5285 Port Royal Road
Springfield, VA 22161-2171
(703) 605-6000

A Small Aircraft Transportation System (SATS)
Demand Model

NS004S1

Executive Summary

The Small Aircraft Transportation System (SATS) is envisioned to take advantage of technology advances in aircraft engines, avionics, airframes, navigation equipment, communications, and pilot training to make it the new generation of general aviation (GA) that will let people travel from small airports. SATS not only will help to break the gridlock at large commercial airports by diverting traffic to non-hub small airports, it also can generate new air traffic demand as it can reduce the door-to-door time for travels from or to a place close to a small airport. With high speed aircraft, numerous airports, an affordable cost, and easy pilot training, SATS can provide better door-to-door travel time, enhance mobility, and stimulate business activity.

This report explains our SATS demand modeling at the national, airport, and air-space levels. We constructed a series of models following the general systems engineering principle of top-down and modular approach. Our three principal models are the SATS Airport Demand Model (SATS-ADM), SATS Flight Demand Model (SATS-FDM), and LMINET-SATS. SATS-ADM models SATS operations, by aircraft type, from the forecasts in fleet, configuration and performance, utilization, and traffic mixture. Given the SATS airport operations such as the ones generated by SATS-ADM, SATS-FDM constructs the SATS origin and destination (O&D) traffic flow based on the solution of the gravity model, from which it then generates SATS flights using the Monte Carlo simulation based on the departure time-of-day profile. LMINET-SATS, an extension of LMINET, models SATS demands at airspace and airport by all aircraft operations in the United States.

The models presented in this report can be the powerful tools to policy decision makers in air traffic system planning, especially in SATS. The models will help project SATS demands for airports and airspace. The models are built with sufficient parameters to give users flexibility and ease of use to analyze SATS demand under different scenarios. Several case studies are included to illustrate the use of the models, which also are helpful in designing the new air traffic management system to cope with SATS traffic.

The figures we present in this study are not forecasts; they are the results of what-if studies. The models, albeit developed with empirical data fitting and flexibility to change the parameters, are not forecast models themselves. The models, however, are constructed so they can easily hook to the SATS Economic Demand Model (SATS-EDM), which will generate SATS demand forecast from the aircraft performance data and the socioeconomic data about areas surrounding the airports. With SATS-EDM in our model suite, we will have a complete SATS demand forecast model. In the last chapter we include our preliminary thoughts on how to construct SATS-EDM.

Contents

Chapter 1 Modeling Framework	1-1
Chapter 2 SATS Airport Demand Model.....	2-1
SELECTED AIRPORTS IN THE STUDY	2-1
GA AIRPORT DEMOGRAPHIC AND ECONOMIC DATABASE	2-4
AN ECONOMIC DEMAND MODEL OF AIRPORT GA OPERATION.....	2-6
DEFAULT AIRPORT GA OPERATION MODEL.....	2-9
GA TRAFFIC MEASURES AND THEIR USE IN SATS DEMAND FORECAST	2-12
Chapter 3 SATS Flight Demand Model.....	3-1
THE GRAVITY MODEL OF ORIGIN AND DESTINATION DEMAND.....	3-2
GA FLIGHT PROFILE	3-3
Distance Distributions.....	3-3
Time-of-day Profile.....	3-8
MONTE CARLO SIMULATION OF GA FLIGHT DEMAND	3-10
Chapter 4 LMINET-SATS	4-1
AIRSPACE FOR PISTON-DRIVEN SATS AIRPLANES.....	4-1
Airlines.....	4-1
Special Use Airspace.....	4-3
Mountains.....	4-4
SATS AND ATM STAFFING	4-4
DEFINITION AND OPERATION OF LMINET-SATS	4-6
Considerations for Adding a SATS Underlayer to LMINET	4-7
SATS airports.....	4-12
LMINET-SATS Operations	4-13
RESULTS.....	4-14
An initial exercise.....	4-14
Effects of Improved Strategies.....	4-20
Conclusions	4-23

Chapter 5 Summary and Future Work	5-1
---	-----

References

Appendix A Parameter Estimation of the Gravity Model

FIGURES

Figure 1-1. Top-down, Modular SATS Demand Modeling.....	1-3
Figure 2-1. Lorenz Curve of GA Operations	2-3
Figure 2-3. Airport Operations Model Schematic.....	2-12
Figure 3-1. Distance Distribution of Single-Engine Aircraft	3-4
Figure 3-2. Distance Distribution of Multi-Engine Aircraft	3-5
Figure 3-3. Distance Distribution of Jet-Engine Aircraft.....	3-5
Figure 3-4. Monthly GA Flights	3-10
Figure 4-1. Fuel Burn and Associated Airspeed For Canadair CL600 Regional Jet	4-2
Figure 4-2. Fuel Burn and Associated Airspeed	4-2
Figure 4-3. Variation of Fuel Burn with TAS at FL 180, Embraer E120	4-3
Figure 4-4. Distribution of Distances of 889 IFR Flights of Light Aircraft.....	4-6
Figure 4-5. Thirty nm Zones around LMINET Airports.....	4-7
Figure 4-6. Low-Altitude Sectors for Albuquerque Air Route Traffic Control Center	4-7
Figure 4-7. Geographic Enroute Sectors	4-8
Figure 4-8. Enroute Sector Structure For Light-Aircraft SATS Operations	4-9
Figure 4-9. FAA High-Altitude Sectors.....	4-9
Figure 4-10. Example Trajectory	4-10
Figure 4-11. SATS Airports.....	4-13
Figure 4-12. Hourly SATS Departures Required to Meet 1 Percent of RPM Demand	4-15
Figure 4-13. Piston ILS Arrivals at Van Nuys, California.....	4-15
Figure 4-14. Piston ILS Arrivals at Morristown, New Jersey.....	4-16
Figure 4-15. Hourly Demand For Busy Sectors, 2007.....	4-18
Figure 4-16. SATS TRACON Demands, 2007.....	4-18
Figure 4-17. Hourly Demand For Busy Sectors, 2022.....	4-19
Figure 4-18. SATS TRACON Demands, 2022.....	4-19
Figure 4-19. Hourly Piston-SATS Arrivals to SATS Airports Near EWR.....	4-20

Figure 4-20. SATS Operations to Supply RPM Deficit..... 4-21

Figure 4-21. Piston-SATS Arrivals to VNY, Deficit Case 4-21

Figure 4-22. Arrivals to Sector 205..... 4-22

Figure 4-23. Arrivals To SATS Airports Near EWR, Deficit Case 4-22

TABLES

Table 2-1. Airport Activity Distribution 2-2

Table 2-2. Top 10 GA Operations Airports 2-3

Table 2-3. Airport Demographic and Economic Database 2-5

Table 2-4. Total Itinerant Landings by Category and Region..... 2-10

Table 2-5. Number of Aircraft by Category and Region 2-11

Table 2-6. Aircraft Utilization Rate by Category and Region 2-11

Table 2-8. Actual Use GA and AT Hours Flown in 1998..... 2-14

Table 2-9. Total TPM by Engine Type and Traffic Distribution in 1998 2-14

Table 2-10. Percentage of Total Operations Flown by Aircraft Type in 1998 2-14

Table 2-11. Constrained and Unconstrained RPM (Billion) Forecasts..... 2-15

Table 2-12. Additional SATS Operations for 1 Percent of Commercial RPM..... 2-15

Table 2-13. Additional SATS Operations to Fill the Gap of Unsatisfied Commercial
Traffic..... 2-15

Table 3-1. Percentiles of Average Daily GA Operations at TAF Airports 3-1

Table 3-2. Samples of ETMS Data in the Distance Distribution Estimation..... 3-4

Table 3-3. Distance (nmi) Statistics for Combined Data Sets..... 3-6

Table 3-4. Model Parameters for Weibull Distribution 3-6

Table 3-5. Estimated Distance (nmi) Statistics Using a Weibull Distribution..... 3-6

Table 3-6. Time-of-day Probability Distribution Function Used in the Simulation 3-9

Chapter 1

Modeling Framework

The transportation system is a vital part of a dynamic economy. For centuries, cities and economies have developed at seaports and along riverbanks, at the railroad and interstate highway intersections, and more recently near airports. Since the first flight made by the Wright brothers about a century ago, the air transportation industry has matured. It has developed from a means of delivering mail to a means of travel for the rich to today's necessary means of travel for conducting business and pursuing leisure. In the United States alone in 2000, there were more than 670 million enplanements and more than 670 billion RPMs. Commercial air transport service has become so important to our business activity and our lives that any disturbance in its service by inclement weather or inadequate air traffic capacity is met by public outcry.

Because of the imbalance of increasing air traffic demand and the relatively constant air traffic capacity, air traffic congestion will become worse. Studies have concluded that our National Airspace System (NAS) will reach gridlock in about a decade, precluding reliable commercial air transport unless demand is curtailed. The more realistic prediction is that airlines will raise ticket prices to curb demand from marginal travelers and curtail operations to remain within the air traffic capacity. These measures will be at the expense of national business activity and the general consumer welfare.

Because travel demand is positively related to population and per capita income, our air travel demand will increase with growing population and economy [1, 2]. Our propensity of air travel, in the meantime, will also be increasing. The Baby Boomer generation will retire with the money and time to travel. The value of human time is increasingly valuable in the fast-paced information age. The economy demands that goods are manufactured and delivered "just-in-time."

Small Aircraft Transportation System (SATS) provides alternatives in air travel—more frequent flights of small aircraft take off and land at small airports. The recent advances in engines, avionics, airframe, navigation, communication, and pilot training have made a new generation of general aviation (GA) possible. SATS will take advantage of the vast pool of small airports to break the gridlock of air traffic congestion.

Air traffic congestion is mostly airport induced, either from insufficient runways, taxiways, gates, or insufficient airspace capacity around airports [3]. The United States has more than 5,000 airports and about 12,000 landing strips, but only about 200 airports have jet operations. SATS will help break the gridlock at large commercial airports by diverting traffic to small airports. It also can pick up latent

air traffic demand because it can speed up door-to-door trip time. With high speed, numerous available airports, affordable costs, and easy pilot training, SATS can provide better door-to-door travel time, enhance mobility, and stimulate business activity.

This report explains SATS demand modeling. SATS is still in its formative stage, but many current generation GA aircraft such as the Cirrus-20 already have SATS technical capabilities. Compared with current GA, SATS may

- ◆ change the speed of travel time and the reaches of destinations;
- ◆ alter avionics requirements for airport and airspace operations; and
- ◆ reduce operating costs and certification requirements.

Other factors will influence SATS operations. Pressurized cabins will enable SATS to fly at higher altitudes, requiring different air traffic control (ATC) service and different air traffic management (ATM) schemes. SATS can be treated as GA with different attributes, which our model will address. Our model will be flexible to account for retrofitting of current GA aircraft, modified attributes, or different percentages of aircraft that have SATS attributes. With this flexibility, our SATS model is a GA model, and we will use SATS and GA interchangeably in our modeling.

GA aircraft are classified¹ as

- ◆ single-engine IFR,
- ◆ single-engine VFR,
- ◆ multi-engine VFR,
- ◆ multi-engine piston IFR,
- ◆ multi-engine turbo IFR, and
- ◆ jet.

Engine types determine the speed and reaches of an aircraft; avionics equipment (VFR/IFR) determine airport and ATC sector demands under different weather conditions. Jets always are assumed to be IFR because flight altitude requires IFR flights.

¹ Helicopter operations are not included in this report's demand modeling because (1) airports are not required for take off and landing and (2) most helicopter operations are VFR, and thus result in few recorded flight tracks. We can capture only a few IFR helicopter flights a day in our ETMS data source.

Figure 1-1. Top-down, Modular SATS Demand Modeling

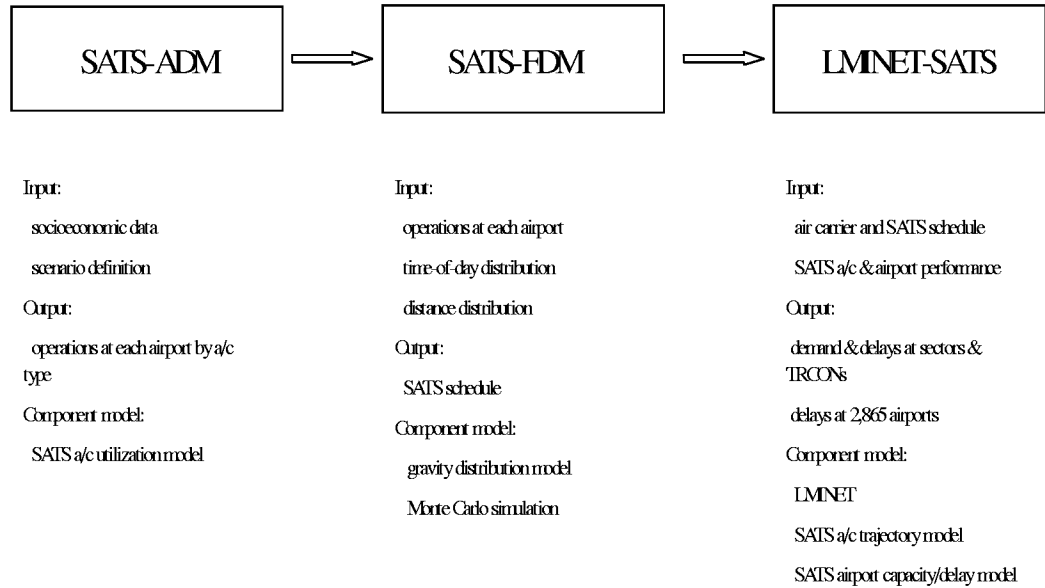


Figure 1-1 shows our SATS demand model built in a top-down, modular fashion following the general system engineering principle. There are three major component models with the following functionalities:

- ◆ SATS Airport Demand Model (SATS-ADM)
 - Input—demographic and economic data, airport and aircraft performance data;
 - Output—annual number of operations by airport and aircraft type;
- ◆ SATS Flight Demand Model (SATS-FDM)
 - Input—output of SATS-ADM;
 - Output—GA flight schedule for entire GA airport network;
- ◆ LMINET-SATS
 - Input—output of SATS-FDM
 - Output—ATC-sector demand for the entire NAS.

From SATS-ADM to SATS-FDM to LMINET-SATS, the GA demand is more and more detailed. The models are linked through input and output, which are common traffic measures used. Each model exists in its own right, and users can substitute them by using best-available information.

Chapters 2, 3, and 4 explain our three principal models, SATS-ADM, SATS-FDM, and LMINET-SATS. Each model has its own subcomponent models. Chapter 5 summarizes model capabilities and identifies future work. The appendixes list technical details of our model.

Chapter 2

SATS Airport Demand Model

SELECTED AIRPORTS IN THE STUDY

There are more than 5,000 airports and approximately 12,000 landing strips in the United States. The most comprehensive databases about these airports are the FAA's Terminal Area Forecast (TAF) and the National Plan of Integrated Airport Systems (NPIAS). For each of the approximately 3,000 airports in the database, TAF maintains information about enplanements, operations, and based aircraft. Of the remaining 2,000 airports not included in the databases, about 1,000 are privately owned but available for public use. Another 1,000 airports are publicly owned but lack sufficient facilities, or do not have sufficient based aircraft, or are within 20 miles of a TAF airport [9].

In the NPIAS, airports (see Table 2-1) are classified as follows:

- ◆ Large hub—enplanement is more than 1 percent of the total U.S. enplanement;
- ◆ Medium hub—enplanement is more than 0.25 percent but less than 1 percent;
- ◆ Small hub—enplanement is more than 0.05 percent but less than 0.25 percent;
- ◆ Nonhub primary—enplanement is more than 10,000 but less than 0.05 percent of the U.S. total;
- ◆ Other commercial—enplanement is more than 2,500 but less than 10,000 annually; and
- ◆ Reliever—GA airports located close to major metropolitan areas.

Table 2-1. Airport Activity Distribution

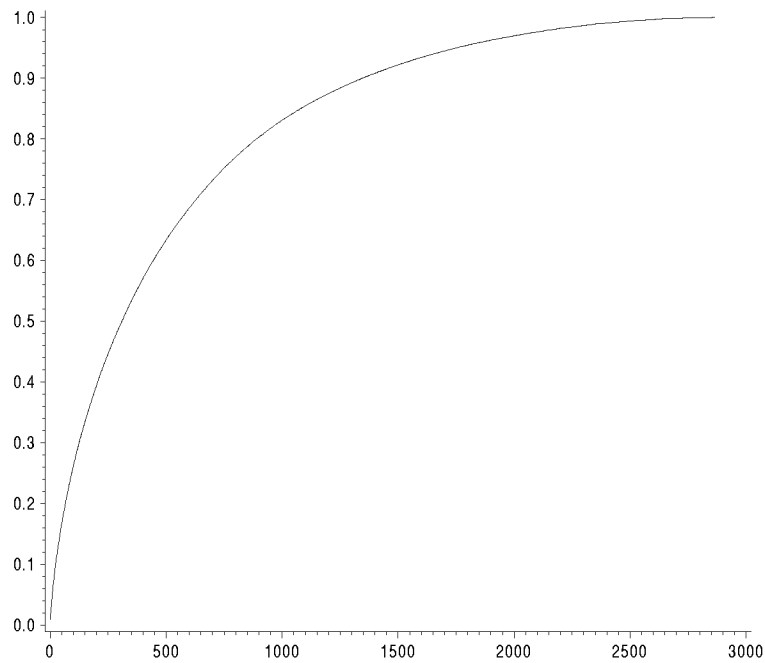
Airport type	Number of airports	Percentage of all enplanements	Percentage of active GA aircraft
Airport type	Number of airports	Percentage of all enplanements	Percentage of active GA aircraft
Large hub	29	67.3	1.3
Medium hub	42	22.2	3.8
Small hub	70	7.1	4.7
Nonhub primary	272	3.3	11.4
Other commercial	125	0.1	2.1
Reliever	334	0.0	31.5
Other GA	2,472	0.0	37.3
TAF	Total 3,344	100.0	92.1

Source: NPIAS.

TAF airports cover 98 percent of the domestic U.S. population within 20 miles of airport radii. The airports are distributed roughly one per county in rural areas and often are located near the county seat. Of all TAF airports, 95 percent are considered to have good or fair runway pavement. We selected the entire database of TAF airports for our study because they cover almost the entire domestic U.S. population and serve current GA activity. Including additional airports does not offer sufficient benefits to justify the substantial effort required to collect additional airport data. With a selection of a smaller set of total TAF airports, it is still possible for us to construct a sound model; however, it is not worth the additional effort required to study out-of-network SATS traffic. If we select all TAF airports, we can ignore all out-of-network traffic as practically insignificant.

We have a network of 2,865 airports after excluding airports in Alaska, Hawaii, Puerto Rico, and Guam. If we rank those airports according to their itinerant GA operations and plot them with the airport distribution, a Lorenz curve results, as shown in Figure 2-1 [5].

Figure 2-1. Lorenz Curve of GA Operations



From this curve, we see that GA operations are concentrated. In fact, 100 airports account for 25 percent of GA itinerant operation, 300 airports account for about 50 percent, and 1,000 airports account for about 83 percent. Table 2-2 lists 10 airports with the most itinerant GA operations in 1997.

Table 2-2. Top 10 GA Operations Airports

Airport	Itinerant GA Operations in 1997
VNY	373,781
SNA	156,216
DAB	232,059
LGB	221,046
APA	197,230
RVS	185,121
FTW	183,301
BFI	182,124
OAK	175,294
FXE	174,142

If we use 600 nmi radius as a criterion that an airport can reach by GA, then an airport in our SATS airport network can reach between 257 to 1,708 airports. The median number of airports that an airport can reach is 1,038. The range of the first quartile and the third quartile is from 643 to 1,347. Any airport in the SATS network has a good number of other airports within its reach.

There is a slight negative correlation between the airport reach and the itinerant operation. The Spearman correlation is -0.12514 [5]. We think this negative correlation is caused by some airports in California, which, because of their geographic location, have limited number of airports among their reach but have large number of GA operations. Thus, we can say that the GA operation at one airport generally does not depend on the number of airports among its reach, but more on the characteristic of its reach.

GA AIRPORT DEMOGRAPHIC AND ECONOMIC DATABASE

The GA Airport Demographic and Economic Database is used to extrapolate economic and demographic information from the current baseline year (1998) to the two future target years (2007 and 2022). A set of reference parameters can be calculated from the 1998 data. Projections are scaled from these reference parameters. For example, one set of parameters is scaled on total household income, then projected to total household income in the future target years.

The database starts with census track data mapped for 3,320 official FAA monitored U.S. airports. The FAA assigns each airport a unique three-letter airport identifier.

The database also includes geographic information for region and state, and hub or reliever status. The important information regarding airport aviation status includes enplanements, based aircraft, and operations.

The term, “enplanement” refers to one passenger boarding an aircraft; distance flown and purpose are not relevant. There are five categories of enplanements: air carrier, air taxi, commuter, U.S., and total. Because enplanement applies to commercial transportation only, numerous airports report zero enplanements across all categories.

“Based aircraft” refers to the number of aircraft, by type, located at an airport. The aircraft types are single engine, multi-engine, jet engine, helicopter, other, and total based aircraft. Because commercial aircraft are never based in any airport, the reported based aircraft are GA or air taxi only.

“Operation” is defined as either an aircraft takeoff or landing. Operations can be classified by purpose. Operations can be itinerant (place to place) or local. The type of aircraft is military, general aviation, air taxi, or air carrier. Categories for

operations are air carrier itinerant, air taxi itinerate, general aviation itinerate, military itinerant, general aviation local, military local, and total operations. (There are no local air carrier or local air taxi operations).

Table 2-3. Airport Demographic and Economic Database

Description	Variable Name
Location id	Locid
Region	Region
Airport Name	Airport
City	City
State	State
Year	Year
Hub Size	Hub Size
Reliever	Reliver
Air Carrier Approaches	AirC App
Air Taxi Approaches	AirT App
General Aviation Approaches	GA App
Military Approaches	Mil App
Total Approaches	Tot App
Single Engine Based Aircraft	SEB Air
Jet Engine Based Aircraft	JEB Air
Multi Engine Based Aircraft	MEB Air
Helicopter Based Aircraft	HelB Air
Other Based Aircraft	OthB Air
Total Based Aircraft	TotB Air
Air Carrier Enplanements	AC Enpla
Air Taxi Enplanements	AT Enpla
Commuter Enplanements	Co Enpla
US Flag Enplanements	US Enpla
Foreign Flag Enplanements	Fo Enpla
Total Enplanements	To Enpla
Primary Air Carrier Overs	Pr AC Ov
Primary Air Taxi Overs	Pr AT Ov
Primary General Aviation Overs	Pr GA Ov
Primary Military Overs	Pr Mi Ov
Secondary Air Carrier Overs	Se AC Ov
Secondary Air Taxi Overs	Se AT Ov
Secondary General Aviation Overs	Se GA Ov
Secondary Military Overs	Se Mi Ov
Instrument Operations Total Overs	InOps TO
Total Instrument Operations	Totl Ops
Air Carrier Itinerant Operations	ACIt Ops
Air Taxi Itinerant Operations	ATIt Ops
General Aviation Itinerant Operations	GAIt Ops

*Table 2-3. Airport Demographic and Economic Database
(Continued)*

Description	Variable Name
Military Itinerant Operations	Milt Ops
General Aviation Local Operations	GAL Ops
Military Local Operations	MiL Ops
Total Operations	Tot Ops
Population In All Rings	Pop All
Population Ring 1 (Red)	PopRing1
Population Ring 2 (Green)	PopRing2
Population Ring 3 (Blue)	PopRing3
Households In All Rings	House All
Households Ring 1 (Red)	HouseRg1
Households Ring 2 (Green)	HouseRg2
Households Ring 3 (Blue)	HouseRg3
Total Household Income In All Rings	TtHsIn
Total Household Income Ring 1 (Red)	TtHsIn1
Total Household Income Ring 2 (Green)	TtHsIn2
Total Household Income Ring 3 (Blue)	TtHsIn3
Average Household Income In All Rings	AvHsInTT
Average Household Income Ring 1 (Red)	AvHsInR1
Average Household Income Ring 2 (Green)	AvHsInR2
Average Household Income Ring 3 (Blue)	AvHsInR3

It is believed in NPIAS that 20 miles radius is a good measure surrounding an airport because it corresponds about 30 minutes driving to the airport. The region surrounding an airport is divided into three rings in the database: the first ring is within 10 miles of the airport; the second ring is from 10 to 20 miles from the airport; and the third ring is 20 to 50 miles from the airport. Some overlap exists between airports (i.e., a household may lie inside the rings of multiple airports). For each defined ring, the database contains population, number in a household, and total and average household income.

The following sections in this chapter discuss database use and its importance in our airport GA operation demand modeling.

AN ECONOMIC DEMAND MODEL OF AIRPORT GA OPERATION

In this section, we build a model of GA operations based on current observations of socioeconomic variables. Current GA travel is not the SATS travel envisioned for the future, although the current GA aircraft, especially corporate jets and those operated in the timeshare program, certainly are SATS-capable. Our construction

of a current GA demand model can offer valuable insight into the SATS demand model.

Because the SATS forecast eventually must be at the airport level, the best data source is our Airport Demographic and Economic Database. According to NPIAS, this data set covers about 98 percent of the total U.S. population, which lives within 20-mile radii of the airports, or about 30 minutes of driving time to an airport.

The linear model is the simplest because the GA traffic is proportional to the surrounding population, although the proportions may be different for the three surrounding rings. For each airport, the following GA demand model is always true:

$$GA = \sum_{i=1}^3 \alpha_i \cdot PopRing_i, \quad [Eq. 2-1]$$

where GA is the measure of GA traffic to be specified, and $\alpha_1, \alpha_2, \alpha_3$ are the parameters that measure the estimated propensity of the population to travel GA. If we think the propensity for GA travel is linearly related to the average household income, i.e.,

$$\alpha_i = \delta_i + \beta_i \cdot AvHsInR_i, \quad i = 1, 2, 3, \quad [Eq. 2-2]$$

then the GA traffic can be rewritten as

$$GA = \sum_{i=1}^3 (\delta_i \cdot PopRing_i + \beta_i \cdot PopRing_i \cdot AvHsInR_i). \quad [Eq. 2-3]$$

This is a linear model if we treat the products of $PopRing_i$ and $AvHsInR_i, i=1, 2, 3$, as separate variables. We think this model probably works only for the GA airports when the large, medium, and small hub airports are excluded, because hub airports are developed for commercial service. To further account for the some of the uniqueness GA airports have to attract travel demand, the GA operations must be related to commercial and air taxi traffic. Our GA demand model can be written as

$$GA = \sum_{i=1}^3 (\delta_i \cdot PopRing_i + \beta_i \cdot PopRing_i \cdot AvHsInR_i) + Ac_Enpla + AtIt_Ops. [Eq. 2-4]$$

If we use the itinerant GA operations as the measure of GA traffic in the above linear regression equation, then we can estimate the parameters. Based on 1998 data, R^2 is about 30 percent¹. This is not a terrible model, but it is not a terrific model either.

¹ R^2 is a goodness-of-fit of the model to the data, which measures as a percentage the variability of the observed data that can be explained by the model.

One cause of the lack of goodness-of-fit is the location of the airports. When we run the same model by region, where each of the nine regions has its own separate parameter estimates, then the R^2 s range from 30 percent through 60 percent. This is an improvement of the model, although the basic idea—that GA traffic is determined by population and average income—is unchanged.

When we run the model by state, the R^2 s range from 30 percent through 80 percent, with model improvement at the high end of R^2 but not at the low end. This means the airports are not homogenous enough at regional or state levels for GA traffic at an airport to be explained by the surrounding population and its average income and location.

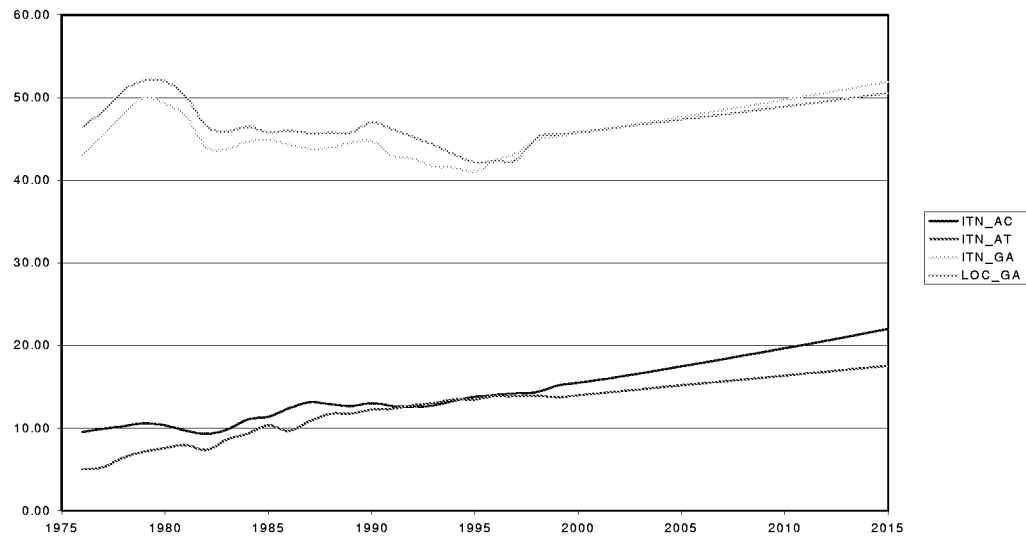
The general idea of this model is good, and model goodness of fit improves when we further classify airports geographically. With additional information about an airport's equipage, access, weather statistics, and surroundings including income distribution and business activities, the model can be improved.

Additional information about an airport and its surroundings does not change our basic assumption that GA traffic is related to the surrounding population whose propensity for GA activity is related directly to its income. Additional information will improve the GA demand model. With more information about the airport, we will need to construct an airport-specific GA demand model (i.e., each airport demand model will have its unique parameters).

Can we construct airport-specific GA demand models based on our GA Airport Demographic and Economic Database? The answer seems to be “no.” First, we have only a few historical data points for 1980, 1990, and 1998 for each airport, which makes the estimation impossible. Even with more data points for each airport, we cannot use all the data because of the structural change in the GA industry since enactment of the GA Revitalization Act in 1994.

Figure 2-2 shows historical and forecast traffic in the 3,320 airports in FAA's 1999 TAF. In the figure, ITN_AC, ITN_AT, ITN_GA, and LOC_GA, are the operations of air carrier, air taxi, itinerant GA, and local GA. The data from 1976 through 1998 are based on observed counts; data beyond 1998 are forecasts. Reversal of the GA traffic decline since enactment of the General Aviation Revitalization Act in 1994 clearly shows the structural change on GA traffic, which reveals the dependence of GA traffic demand on the government policy. From this we can further infer that the SATS demand will also depend on the government policy, or more broadly, on the general SATS operation environment. The difficulty to predict the government policies makes the SATS demand forecast even more difficult.

Figure 2-2. Total Observed and Forecast Operations in TAF Airports



Source: Terminal Area Forecast, FAA

In conclusion, it is good experience to try to construct a current GA demand model. What we have learned though the GA modeling can be applied to the SATS modeling:

- ◆ SATS demand should be directly related to the surrounding population.
- ◆ Propensity for SATS travel is directly related to the household income of the population surrounding an airport.
- ◆ The SATS demand model should be airport specific (i.e., with unique sets of parameters in the same model structure).

DEFAULT AIRPORT GA OPERATION MODEL

Different aircraft have different performance capabilities for speed, range, and altitude, and different avionics equipment determines what ATC service they require and where they can go in different conditions. This detailed information is required by LMINET-SATS to build an accurate picture of ATC demand from SATS. For the SATS-ADM, we must generate airport itinerant operation by single, multi, or jet engine type.

For each airport, TAF forecasts the number of based aircraft in the categories of single engine, multi-engine, jet, helicopter, and other; and itinerant operations conducted by air carrier, air taxi, and GA; and local GA operations. Our main task in this section is to have a model by aircraft type for itinerant traffic. Because all GA aircraft need similar airport services, we do not further decompose local GA traffic to different categories.

By the nature of its service and lack of further information, we assume the aircraft categorical composition of air taxi is the same as GA. For our 2,865 SATS airport network, the averages of itinerant GA and air taxi operations per airport in 1998 are 14,644 and 4,308, respectively. In other words, the air taxi category accounts for about 22 percent of the combined itinerant operations. The slight difference between GA and air taxi categorical composition will not make a big difference in our model because GA contributes most traffic.

An airport's itinerant operation comes from two sources: one from locally based aircraft, the other from aircraft from the outside. Operations by locally based aircraft are directly proportional to the locally based fleet multiplied by its utilization rate. The utilization rate is defined as the number of itinerant operations conducted by one aircraft per year. Lacking other information, we assume the operations conducted by outside-based aircraft based outside are proportional to the traffic mix surrounding the airport.

General Aviation and Air Taxi Association (GAATA) database contains the most detailed information about GA and air taxi itinerant operations at the regional level. Because we know the location and based aircraft by category for each airport in TAF, we can directly compute aircraft utilization by dividing total regional itinerant operations by total aircraft based in the region. We assume all itinerant operations are conducted intra-regionally. Table 2-4 shows the number of itinerant landings in 1997 by region based on GAATA.

Table 2-4. Total Itinerant Landings by Category and Region

Region	Single	Multi	Jet	Other
ACE	520,933	290,625	52,546	15,729
AEA	746,220	208,981	160,411	48,897
AGL	1,177,271	640,879	372,910	77,090
ANE	363,309	81,865	20,065	33,177
ANM	646,049	257,036	53,656	51,690
ASO	1,066,159	616,792	254,729	63,216
ASW	913,787	332,008	139,623	54,671
AWP	1,123,728	290,260	70,953	67,318

Table 2-5. Number of Aircraft by Category and Region

Region	Single	Multi	Jet	Other
ACE	7,586	1,347	413	367
AEA	14,512	2,783	872	1,310
AGL	22,652	4,150	1,158	1,174
ANE	5,082	705	159	295
ANM	15,126	1,947	429	805
ASO	21,503	5,749	1,394	1,231
ASW	15,853	3,426	1,313	856
AWP	29,453	4,235	763	808

Table 2-6. Aircraft Utilization Rate by Category and Region

Region	Single	Multi	Jet	Other
ACE	68.67	215.76	127.23	42.86
AEA	51.42	75.09	183.96	37.33
AGL	51.97	154.43	322.03	65.66
ANE	71.49	116.12	126.19	112.46
ANM	42.71	132.02	125.07	64.21
ASO	49.58	107.29	182.73	51.35
ASW	57.64	96.91	106.34	63.87
AWP	38.15	68.54	92.99	83.31

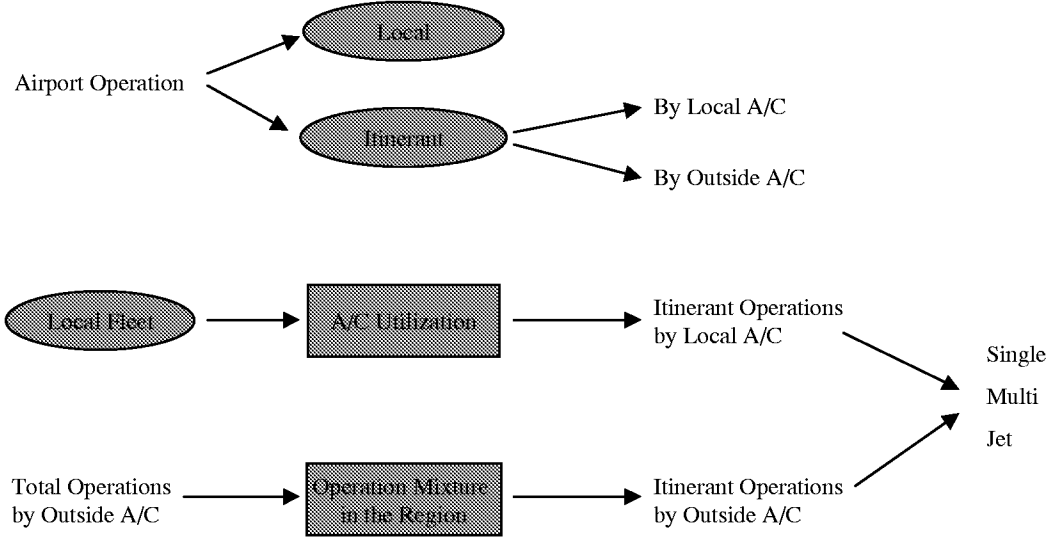
We assume the aircraft utilization rates are stable in the default forecast. In using the model, the analyst has the flexibility to use any utilization rates at any airport. After the analyst selects the utilization rates, the number of annual itinerant landings is attained by multiplying the fleet by its utilization rate. The regional landing distribution by aircraft and region changes based on the distribution of aircraft in the region. Table 2-7 shows the 1998 landing rates by aircraft and region.

Table 2-7. Distribution (%) of Landings By Category and Region in 1998

Region	Single	Multi	Jet	Other
ACE	59.21	33.03	5.97	1.79
AEA	64.08	17.95	13.77	4.20
AGL	51.90	28.26	16.44	3.40
ANE	72.89	16.43	4.03	6.66
ANM	64.06	25.49	5.32	5.13
ASO	53.28	30.83	12.73	3.16
ASW	63.45	23.05	9.70	3.80
AWP	72.39	18.70	4.57	4.34

At each airport, the difference of the total itinerant operations given by the default FAA TAF and the operations conducted by the locally based aircraft computed by multiplying the fleet by its utilization rate, is the total operations by visiting aircraft, which follow the regional distribution of the airport. Figure 2-3 is a schematic of the model.

Figure 2-3. Airport Operations Model Schematic



After all itinerant operations at an airport are fully decomposed, the “other” category is distributed proportionally to the categories of single-engine, multi-engine, and jet.

GA TRAFFIC MEASURES AND THEIR USE IN SATS DEMAND FORECAST

While the default GA operations model described in the previous section will enable us to find the operations of each aircraft type for each airport based on the default forecast in the FAA’s TAF, the model to be developed in this section will let us predict future SATS, or additional GA demand. We follow the system engineering modeling principle to have a series of component models to generate measurable, easy-to-change GA traffic measures. Primary data sources are the TAF, GAATA, and Airport Demographic and Economic Databases outlined in this chapter. Two case studies are included to illustrate the methodology and the traffic measures in the “what-if” scenarios that show SATS picking up some portion of unsatisfied commercial traffic demand.

Many statistics such as operation and enplanement are available to measure commercial air traffic, but the most important one is RPM. RPM encompasses operation and enplanement, and, more importantly, it is closer to measure the purpose of air traffic—moving people from one place to another. GA traffic has been

measured only by its operations, while enplanement and RPM have never been measured and reported. There are reasons not to report them. First, unlike commercial traffic, there is no mechanism to report GA flight passengers’ origin and destination. Second, GA flight lacks the concept of revenue passenger; at times, a GA flight has no passenger, only a pilot.

SATS will share the same kind of operation as the current GA; it also will share the same difficulty in reporting its traffic statistics. SATS, nonetheless, is envisioned to fulfill the transportation need of moving people from one place to another. It is unavoidable then to define a similar measure like RPM in commercial traffic for SATS or GA. In this case, a transported passenger may not pay for the flight or may be the pilot, as long as he or she takes SATS to fulfill the transportation need of moving from one place to another. Here we will use the term “*Transported Passenger Mile*” (*TPM*) in lieu of RPM . Following the same definition for the commercial traffic, TPM for a SATS or GA flight is defined as follows:

$$TPM = transported_passenger \times flight_distance, \quad [Eq. 2-5]$$

which can be further broken down to

$$TPM = aircraft_size \times load_factor \times distance. \quad [Eq. 2-6]$$

Equation 2-5 provides a practical means of computing TPM. For example, to find the TPM for a category, by aircraft type or by region, one needs to the sum the TPMs of all the flights falling in the category. Table 2-7 lists TPMs and the conversion factors of 1 billion TPM to operation by different engine types.

Table 2-7. Average GA TPM and Equivalent Number of Operations of 1 Billion TRM by Engine Type

Engine type	Seat	Load factor	Distance (mile)	TRM	Operations per 1 billion TRM
Single	4	0.9	261	940	1,064,281
Multi	6	0.8	318	1,526	655,136
Jet	8	0.7	909	5,090	196,488

In Table 2-7, the average distance is based on our data analysis of Instrument Flight Rule (IFR) flights recorded in ETMS, while the seats and load factors are the ones we assume reasonable based on aircraft type. The table gives a clear view of TPMs and how they relate to seat, load factor, and distance, which the user can modify. The last column in the table is the equivalent number of operations, calculated using Equation 2-6. This is important because it translates the SATS traffic measured in TPM to operation, which will be useful for airport planning and our construction of SATS FDM.

It is more efficient to carry SATS traffic in jet aircraft per operation, as seen in the conversion factor column—more passengers can be carried a longer distance per

flight. The ultimate decision—which SATS flight a transported passenger will take—will depend on many factors: operating cost, aircraft equipage, trip mission, airport facilities, etc. Because SATS aircraft can be different in engine types, a SATS demand distribution model is needed to decompose overall demand into different categories. Such a model is constructed using GAATA data.

Table 2-8. Actual Use GA and AT Hours Flown in 1998

GA & AT hours	Corporate	Business	Personal	Other work	Air taxi	Total
Single	212,900	2,192,013	8,044,572	110,455	406,276	10,966,216
Multi	1,015,027	680,278	573,009	18,682	924,827	3,211,823
Jet	1,435,231	24,294	18,864	0	120,592	1,598,981

Data Source: GAATA

Table 2-9 shows distance as airspeed multiplied by flight hour for total TPM for each engine type and the distribution.

Table 2-9. Total TPM by Engine Type and Traffic Distribution in 1998

Aircraft type	Total hours	Speed	Seat	Load factor	Total TPM	TPM (%)
Single	10,966,216	178	4	0.9	7,027,151,213	47.62
Multi	3,211,823	262	6	0.8	4,039,188,605	27.37
Jet	1,598,981	412	8	0.7	3,689,168,963	25.00

In the above Table 2-9, we took the total flight hours from the GAATA database. We based the speeds on our estimation of ETMS data. The seats and load factors are our assumptions, and the total TPMs and their distribution just follow the formula. Under our seat and load factor assumptions, the single-engine aircraft carried about half of GA traffic in 1998, while the multi-engine and jet engine aircraft each carried about a quarter of GA traffic. Model users can modify the input parameters or change the traffic allocation. Table 2-10 shows that in operations, the single-engine aircraft is far more dominant.

Table 2-10. Percentage of Total Operations Flown by Aircraft Type in 1998

Aircraft type	%
Single engine	73.1
Multi-engine	10.9
Jet	2.7
Rotorcraft	3.5
Other	9.8

Data source: GAATA.

The remainder of this section presents a case study of a project to determine additional SATS demand if SATS is used to pick up unsatisfied commercial traffic. Table 2-11 shows the constrained and unconstrained RPM forecasts where the unconstrained RPM forecasts are from TAF while the constrained forecasts are based on the integrated ASAC ACIM and the operations models.[2]

Table 2-11. Constrained and Unconstrained RPM (Billion) Forecasts

	Year 2007	Year 2022
Unconstrained	932.7	1,841
Constrained	909.0	1,650
Delta/ RPM gap	23.8	191
Percentage gap	2.6%	10.4%

The gap in the two forecasts is 2.6 percent in 2007; it grows to 10.4 percent in 2022. In real terms, the gaps are about 24 billion RPM in 2007 and 190 billion RPM in 2022.

Two scenarios present interesting cases. The first scenario assumes a small percentage of diversion (we assume 1 percent) from commercial RPM to SATS TPM in the future. In the second scenario, SATS carries all unsatisfied commercial traffic. The two scenarios give the lower and upper bounds of SATS traffic. To calculate additional SATS demand diverted from unsatisfied commercial traffic, we first decompose the traffic by engine type according to Table 2-9. Then we multiply the TPMs for each engine type by the conversion factors in Table 2-7. This yields additional SATS operations by engine type.

Table 2-12. Additional SATS Operations for 1 Percent of Commercial RPM

Year	TPM (billion)	Single	Multi	Jet
2007	9.32	4,727,419	1,672,683	458,104
2022	18.41	9,424,426	3,334,605	913,262

Table 2-13. Additional SATS Operations to Fill the Gap of Unsatisfied Commercial Traffic

Year	TPM (billion)	Single	Multi	Jet
2007	23.8	12,113,789	4,286,171	1,173,871
2022	191.0	105,628,185	37,373,976	10,235,762

In the second scenario, additional SATS represent a 22 percent increase in GA operations beyond the baseline operations in 2007, and a 140 percent increase in operations in 2022.

Additional future GA operations conducted by SATS depend on the scenario and input parameters. Our case studies show that these tables provide useful ways to impute future SATS operations. The tables are constructed for easy understanding, and directly relate to common statistics on air travel and aircraft performance. The tables are populated with current GA traffic information, yet they can be modified to reflect future SATS operations.

Chapter 3

SATS Flight Demand Model

In this chapter, we explain how we constructed an origin-and-destination (O&D) flight demand schedule for GA, which will feed into the LMINET-SATS to compute airport and airspace demand. “GA schedule” does not mean that the GA operations will be scheduled; rather, it is an expression of the GA flight in terms of O&D and time. The analysis presented in this section is based on the given airport operation figures such as the one developed in Chapter 2.

While it is tempting to construct the future GA demand schedule based on current GA flights, we lack sufficient information about current GA operations and schedules for all flights. The lowest average total daily operations at all TAF airports is zero; the highest average number of daily operations is 1,024. For an airport with about 1,000 operations a day, some hours can have about 100 operations per hour, which is close to the figure for a medium-sized commercial airport. However, typical airports have an average of only 13 operations a day, or about one an hour. Table 3-1 shows the average total itinerant GA operations for all TAF airports in 1998.

Table 3-1. Percentiles of Average Daily GA Operations at TAF Airports

Cumulative distribution (%)	1	5	25	50	75	90	95	99
Percentile	0.0	0.14	4.4	12.6	41.1	95.9	145.9	298.2

GA traffic flow is thin, but GA flights have numerous potential destination airports to land. Within a 600-mile radius of an airport, there can be from 300 to more than 1,500 airports, which means GA flights have far more destination choices than commercial flights. It is not a good idea to assign O&D traffic on the basis of a few observed GA schedules.

Another technical challenge we face is that ETMS is the only data source from which we can extract the GA schedule. ETMS contains only IFR flights, but most GA flights are VFR. For 1998 (the most recent statistics available), there are 5.4 million IFR flight hours for fix-winged aircraft compared to 24.1 million flight hours of all flight plans in the same category. There are 1.6 million IFR flight hours for single-engine piston aircraft compared to 18.3 million flight hours of all flight plans in the same category (see GAATA Table 4-7). In other words, using ETMS will make the GA traffic flow information even thinner to cover greater possibilities of GA or SATS scheduling.

We face two technical problems: (1) the GA operations are low at the airports but broad in the O&D pair; and (2) the GA schedule we can extract represents a small portion of total GA. The technique that we use to construct the GA schedule is to combine the time-of-day departure profile and distance of travel profile with the gravity model to get the O&D distribution, and then use Monte Carlo simulation. When constructing a GA schedule, we will take the stance that departure time is independent of the destination choice, which makes it possible for us to have two separate models for the time-of-day departure profile, and the O&D distribution model.

We assume most GA aircraft can travel just a few hours before refueling. Because the GA schedule is based on these time profiles, and there will be few O&D flights between airports, demand likely will be a fraction of a flight. The Monte Carlo simulation technique will overcome this deficiency by generating integer numbers of flights in the GA schedule based on the probabilities specified by the time-of-day departure profile and O&D distribution model. Many rounds of Monte Carlo simulation must be run and fed into the LMINET-SATS to calculate delays.

THE GRAVITY MODEL OF ORIGIN AND DESTINATION DEMAND

In the simplest form, the gravity model is

$$t_{ij} = m_i^{\alpha_i} \cdot m_j^{\alpha_j} \cdot c_{ij}^{\beta}, \quad i = 1, 2, \dots, N, \quad [\text{Eq. 3-1}]$$

where t_{ij} is the traffic from city i to city j , m_i and m_j are the “masses” of city i and j , respectively, and c_{ij} is the “cost” or the “attractiveness” of traveling from city i to city j . In studies, researchers have used population, per capita income, and other criterion as masses and pecuniary expense or time of the travel as cost. α_i , α_j , and β are the model parameters to be estimated. The gravity model has been used widely in O&D demand modeling. It is called “gravity model” because it mimics the form of Newton’s Gravity Law. The above gravity model can be re-written as

$$t_{ij} = a_i \cdot b_j \cdot T_i \cdot T_j \cdot c_{ij}, \quad i = 1, 2, \dots, N, \quad [\text{Eq. 3-3}]$$

where T_i is the total traffic from i ; T_j is the total traffic to j ; and c_{ij} is the coupling parameter from i to j , which is normally negatively related to the “cost” of travel from i to j or positively related to the attractiveness from i to j . Because the traffic must satisfy the conservation, or

$$\sum_{j \neq i} t_{ij} = T_i, \quad i = 1, 2, \dots, N, \quad [\text{Eq. 3-5}]$$

Then the normalizing constants a_i and b_j must satisfy the following:

$$a_i \sum_j b_j \cdot T_j \cdot c_{ij} = 1, i = 1, 2, \dots, N; \quad [\text{Eq. 3-7}]$$

$$b_j \sum_i a_i \cdot T_i \cdot c_{ij} = 1, j = 1, 2, \dots, N. \quad [\text{Eq. 3-9}]$$

The second form of the gravity model Equation 3-2 offers an advantage when terminal traffic T_i and T_j are known and the task is to estimate the traffic for every O&D pair.

In this model, we propose using the distance probability distribution function for the coupling parameter c_{ij} , i.e.,

$$c_{ij} = f(d_{ij}), i, j = 1, 2, \dots, N. \quad [\text{Eq. 3-11}]$$

On the aggregate level, the distance probability distribution function reflects the propensity people have for travelling on a particular type of aircraft equipment. In ETMS, the origin and destination of a flight are recorded, from which we can compute the flight distance. In running the model, we can assume that both IFR and VFR flights cover the same distance statistically. This is a reasonable assumption because the difference between IFR and VFR is just the avionics equipment. Again, the model is flexible to take any distance profile for any group of aircraft. After selection of the airport pair i and j , we will calculate their distance d_{ij} . Based on the value of d_{ij} and Equation 3-6, we can find the coupling parameter c_{ij} . In running the model, users can opt for their own distance probability function for each category.

Appendix A contains the parameter estimation algorithm of c_{ij} , $i, j \in \{1, 2, \dots, N\}$.

GA FLIGHT PROFILE

Distance Distributions

We need to construct the probability distribution function, based on ETMS, for single engine, multi-engine, and jet equipment categories. We selected 12 ETMS samples, shown in Table 3-2, to include different seasons, days of the week, and times of day.

Table 3-2. Samples of ETMS Data in the Distance Distribution Estimation

Date	Time	Day
6/19/00	0900	MON
6/10/00	1500	SAT
6/10/00	0900	SAT
5/23/00	0900	TUES
5/23/00	1800	TUES
3/29/00	1200	WED
10/1/99	2000	FRI
9/30/99	1200	THURS
9/29/99	1200	WED
9/28/99	1600	TUES
4/16/99	0800	FRI
4/16/99	1200	FRI

Figures 3-1 through 3-3 show histograms of the flight distance for the combined data.

Figure 3-1. Distance Distribution of Single-Engine Aircraft

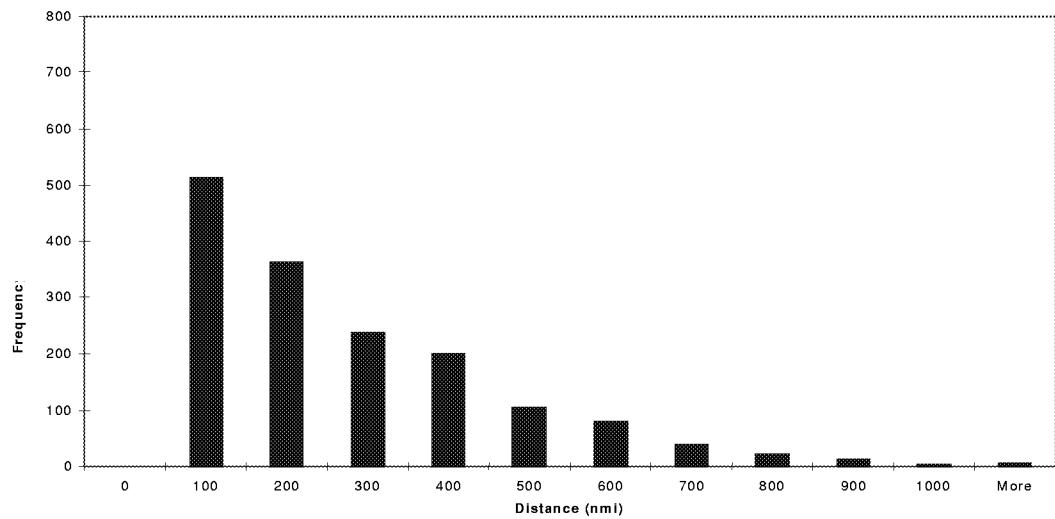


Figure 3-2. Distance Distribution of Multi-Engine Aircraft

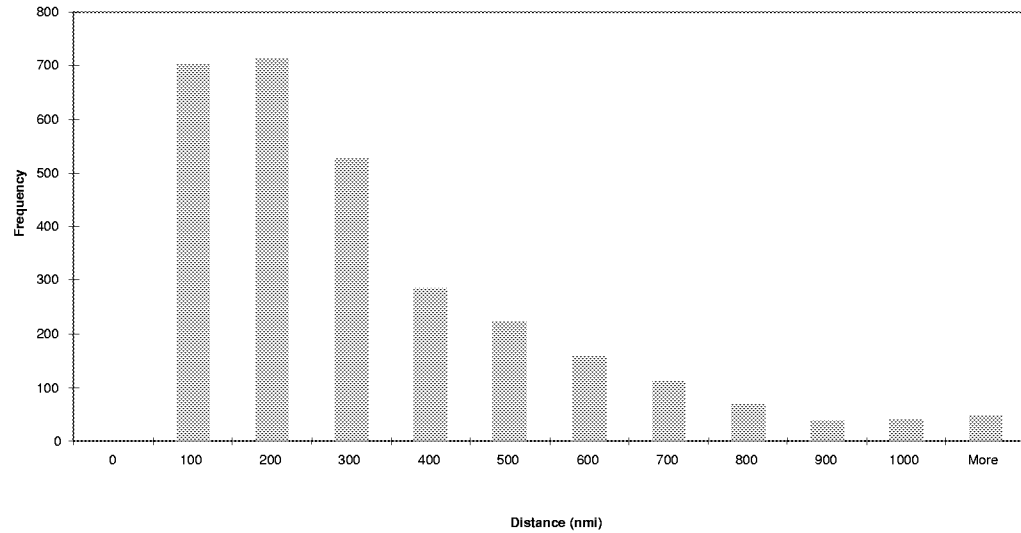
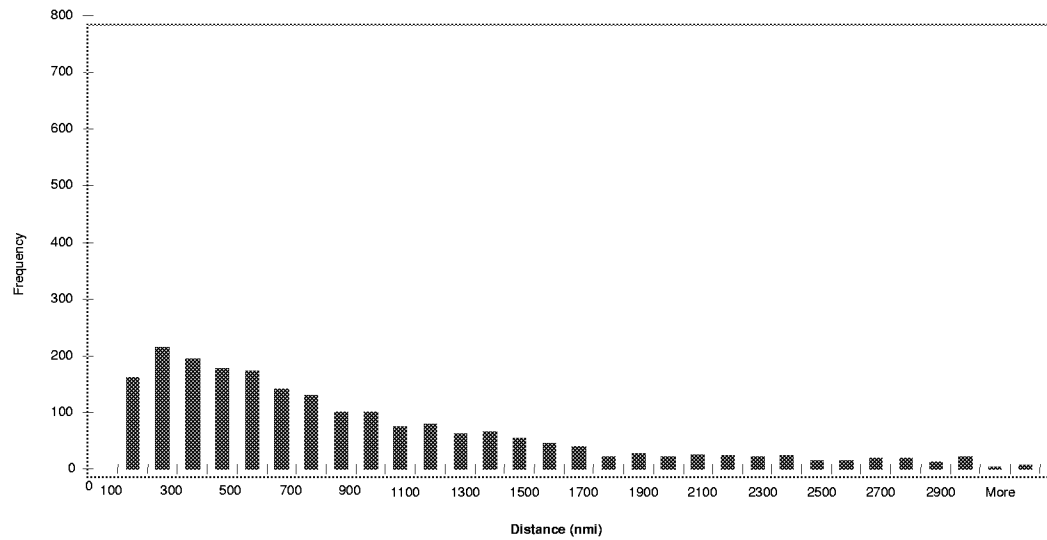


Figure 3-3. Distance Distribution of Jet-Engine Aircraft



Distribution fitting shows that distance traveled according to aircraft engine type (single, multi, and jet) is best modeled by Weibull distribution, whose probability density, and probability cumulative functions in general are as follow:

$$f(x; \delta, \lambda) = \frac{\lambda}{\delta} \left(\frac{x}{\delta}\right)^{\lambda-1} e^{-\left(\frac{x}{\delta}\right)^\lambda}, \quad x \geq 0; \delta, \lambda > 0, \quad [\text{Eq. 3-13}]$$

and

$$F(x; \delta, \lambda) = 1 - e^{-\left(\frac{x}{\delta}\right)^\lambda}, \quad x \geq 0; \delta, \lambda > 0, \quad [\text{Eq. 3-15}]$$

where δ and λ are the Weibull scale and shape parameters, respectively.

We find no statistical significance that the samples are different. The parameters for the combined sample are shown in Table 3-3.

Table 3-3. Distance (nmi) Statistics for Combined Data Sets

	Single engine	Multi-engine	Jet engine
Mean	227.0	276.0	790.0
Std. Dev.	196.0	242.0	684.0
Variance	38,304	58,502	467,807
Skewness	1.66	1.63	1.26
Kurtosis	8.12	6.18	3.99

Table 3-4. Model Parameters for Weibull Distribution

	Single engine	Multi-engine	Jet engine
Scale	237	289	826
Shape	1.15	1.16	1.14

Table 3-5. Estimated Distance (nmi) Statistics Using a Weibull Distribution

	Single engine	Multi-engine	Jet engine
Mean	227.0	277.0	790.0
Std. Dev.	196.0	236.0	691.0
Variance	38,525	55,827	476,866
Skewness	1.61	1.59	1.64
Kurtosis	6.73	6.59	6.82

Thus, based on the estimated parameters, the pdf's for each aircraft engine type are as follows:

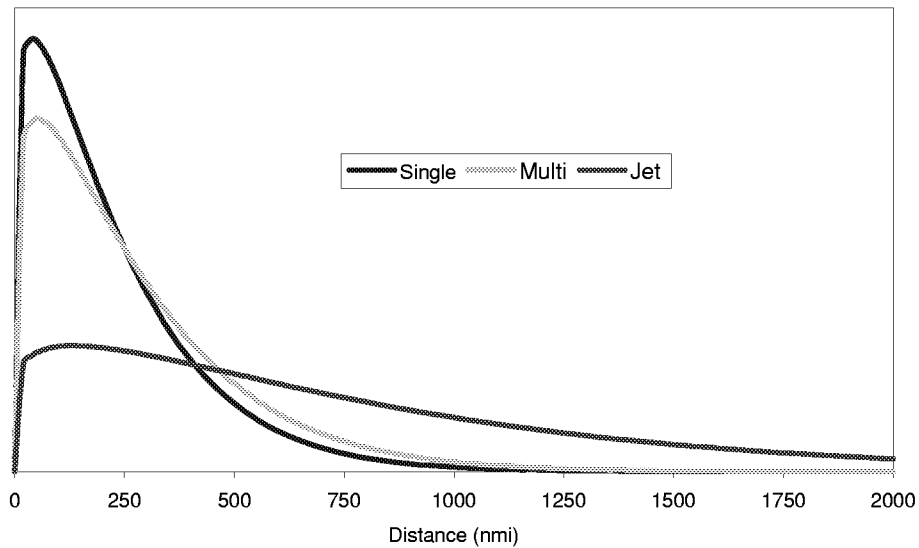
$$f_s(x; \delta_s, \lambda_s) = \frac{1.15}{237} \left(\frac{x}{237} \right)^{0.15} e^{-\left(\frac{x}{237} \right)^{1.15}}, \quad [\text{Eq. 3-17a}]$$

$$f_m(x; \delta_m, \lambda_m) = \frac{1.16}{289} \left(\frac{x}{289} \right)^{0.16} e^{-\left(\frac{x}{289} \right)^{1.16}}, \quad [\text{Eq. 3-9b}]$$

$$f_j(x; \delta_j, \lambda_j) = \frac{1.14}{826} \left(\frac{x}{826} \right)^{0.14}, \quad [\text{EQ. 3-9c}]$$

where f_s , f_m , and f_j are the pdfs for single, multi-, and jet engine aircraft, respectively, which are depicted in Figure 3-4.

Figure 3-4. Probability Density Functions of the Estimated Parameter



The cdfs for each aircraft engine type are as follows:

$$F_s(x; \delta_s, \lambda_s) = 1 - e^{-\left(\frac{x}{237}\right)^{1.15}}, \quad [\text{Eq. 3-19a}]$$

$$F_m(x; \delta_m, \lambda_m) = 1 - e^{-\left(\frac{x}{289}\right)^{1.16}}, \quad [\text{Eq. 3-10b}]$$

$$F_j(x; \delta_j, \lambda_j) = 1 - e^{-\left(\frac{x}{826}\right)^{1.16}}, \quad [\text{Eq. 3-10c}]$$

where F_s , F_m , and F_j are the cdf's for single-, multi-, and jet engine aircraft, respectively.

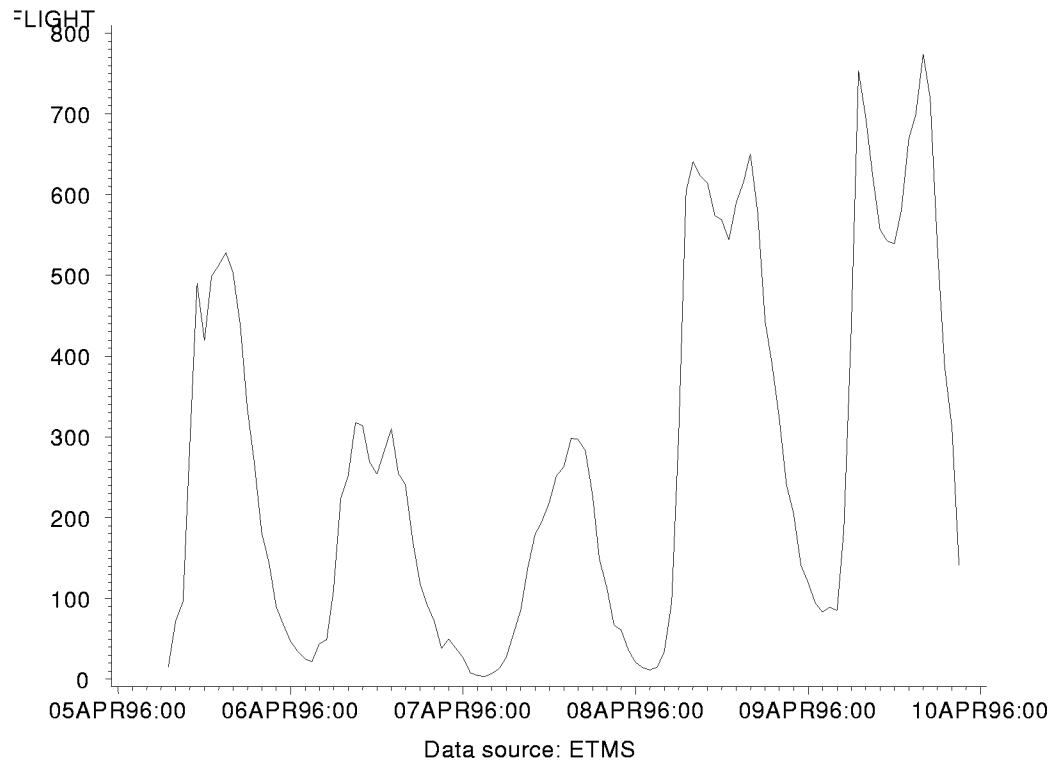
The shape parameters of the estimated Weibull distribution for the three different engine types are so close, their differences are caused mainly by the scale parameter. Because the speeds of the different engine types are different, this may suggest the shape parameter is more universal, relating to more fundamental characteristics of a flight such as the pilot's physical limit of distance required to stop.

We need to construct a similar distance probability function for SATS aircraft for each engine type. We believe the distance probability distribution function depends on the range of the aircraft, and probably more important, on the duration of a flight, attributable to pilots' physical and psychological limits. Because the proposed single-engine SATS aircraft will be capable of higher speed than the current single-engine GA aircraft, the distance probability distribution function will be a stretched version of the current single-engine GA if we want to keep the duration of flight unchanged. We believe there are no significant range or speed differences between the current GA and the proposed SATS in either multi-engine or jet categories.

Time-of-day Profile

The following figure shows the total number of departures recorded in ETMS by the local time for a few days in April 1996.

Figure 3-4. Total Number of GA Departures by Local Time in the United States



There clearly is an hourly departure pattern across the days. In modeling, we assumed that the VFR flights share the same time-of-day departure profile with the IFR flights as recorded in ETMS.

We must convert the total number of departures to the probabilities of the daily total departure based on Figure 3-4. We will use more ETMS data as it becomes available. In the simulation in this report, all airports share the same time-of-day departure probability function, which is estimated by using the GA flight counts recorded by ETMS during April 5–10, 1996. Users can choose their own profile for any airport in the system.

Table 3-6. Time-of-day Probability Distribution Function Used in the Simulation

Time	Prob-ability	Time	Prob-ability	Time	Prob-ability	Time	Prob-ability
0	0.71	6	3.36	12	6.68	18	5.49
1	0.46	7	5.80	13	7.36	19	4.18
2	0.41	8	5.70	14	7.85	20	3.20
3	0.46	9	6.12	15	8.16	21	1.98
4	0.62	10	6.65	16	8.01	22	1.17
5	1.05	11	6.75	17	7.06	23	0.80

MONTE CARLO SIMULATION OF GA FLIGHT DEMAND

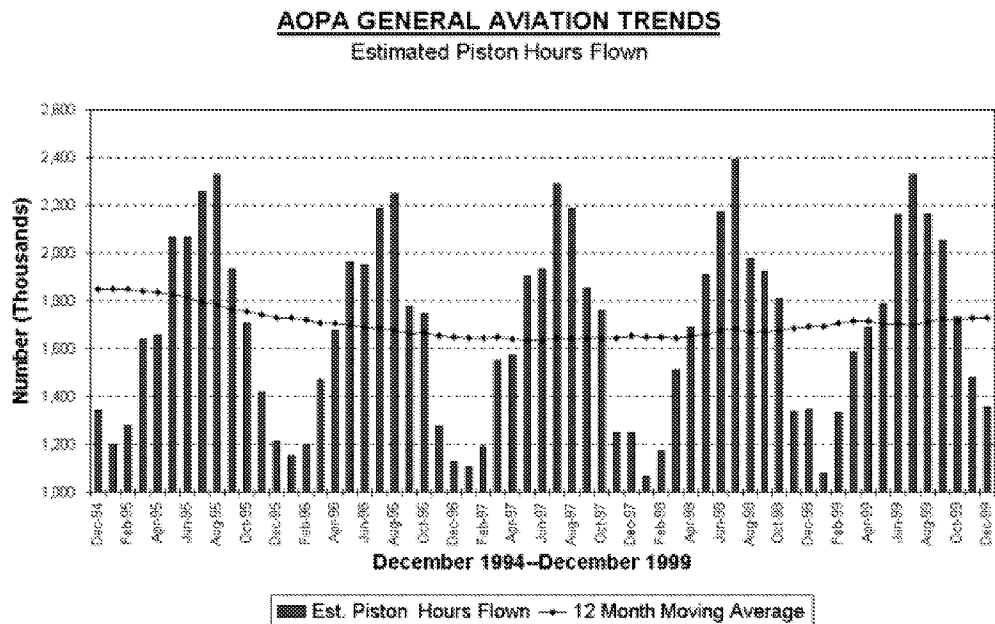
Multiple samples will be needed to counter the randomness. After the samples are created, they will feed into the LMINET-SATS individually. Average delays will be computed for all the sample runs.

One important issue in Monte Carlo simulation is to decide how many flights to generate for one day's "schedule." Instead of using the rigid method of generating a fixed number of flights for each airport distributed according to its destination and time of day, we will generate the entire pool of flights for all airports selected in the network. The advantage of this approach is that the "schedule" generated is more random, and airports with very few operations may not be covered by the schedule for a random day. The total number of flights of one aircraft category in the entire network, N_{Daily} is given as

$$N_{Daily} = N_{Annual-Ops}/365/2*1.5, \quad [Eq. 3-21]$$

where $N_{Annual-Ops}$ is the total annual number of operations in the network, which is twice the number of flights by definition. We multiply the average daily total flights by a factor of 1.5 to simulate the traffic in high season. Figure 3-4 shows the seasonal GA pattern.

Figure 3-4. Monthly GA Flights



We made the following assumptions in the simulation:

- ◆ The selections of aircraft categories are independent, meaning we can conduct the Monte Carlo simulation independently and separately for each aircraft category.
- ◆ The distribution of originating airport, destination airport, and time-of-day are independent among each other, meaning we can generate the originating airport i , destination airport j , and the time k independently and separately.

The schematic of the simulation is as follows:

Repeat 1, 2, 3, and 4 for all aircraft categories

1. Compute the cumulative probability distribution function of the originating airports $O(i)$, based on the forecast annual itinerant operations.
2. Compute the cumulative probability distribution function, for each originating airport, of the destination airport $D_i(j)$, based on the traffic resulting from the gravity model.
3. Compute the total number of flights N_{Daily} based on Equation 3-11.
4. Repeat N_{Daily} times for steps a, b, c, and d.
 - a. Generate originating airport i according to $O(i)$.
 - b. Generate destination airport j according to $D_i(j)$.
 - c. Generate time according to time-of-day distribution function $T(k)$.
 - d. Put the generated GA flight schedule in the appropriate avionics category according to the probabilities.

The generation of a random variable $x \in \{1, 2, \dots, N\}$ according to any cumulative probability distribution function F is done by following two steps:

1. Generate random variable U , which is uniformly distributed in $[0,1]$. Most general-purpose programming languages such as C have built-in functions for this task.
2. x is the smallest number that $F(x) \leq U$.

According to Table 4-7 of GAATA, by hours of flight plan in a 1998 survey, 8.98 percent of single-engines, 58.37 percent of multi-engines, and 93.1 percent of jet engines are IFR, respectively. Further, for IFR multi-engine hours, 50.7 percent is piston, while the rest is turbo-prop. For the Monte Carlo simulation of

the future default GA traffic, we assumed the number of flights of each category follows the same probability of flight hours reported above, except for 100 percent IFR probability for jet engines. With no any direct information about the probabilities of flights themselves, we believe this assumption is a good one if the flight hours for each flight are the same for each engine category regardless of the avionics equipage. Model users can modify those probabilities.

For additional SATS traffic case studies, the GA schedule is the sum of the default schedule and the schedule from the additional SATS. The Monte Carlo simulation of the additional SATS is generated by using the same gravity model parameters as in the default case. For the SATS simulation in the report, while we still keep the same piston multi-engine probability under IFR, we assume the IFR probabilities for all engine categories is 100 percent. We make this assumption because the additional SATS will be used mainly for transportation, which should be wholly IFR to maintain flight reliability. Again, model users can select their probability parameters.

Chapter 4

LMINET-SATS

This chapter explains how we developed a companion utility for LMI's queueing network model of the U.S. National Airspace System (NAS) to model air traffic generated by SATS operations.

SATS operations will use airports that are now unused or underused for air travel, and SATS light airplanes will use airspace that is now little used for transport.

AIRSPACE FOR PISTON-DRIVEN SATS AIRPLANES

Developing LMINET-SATS and understanding its results require an understanding of the airspace that SATS aircraft can use. We assume that turbojet and turbo-prop SATS aircraft will operate at altitudes typical of GA aircraft of the corresponding type. LMINET tracks those its operations. LMINET-SATS must deal with single and multi-engine, piston-driven SATS aircraft.

We assume that piston-SATS aircraft will not be pressurized. Unpressurized SATS airplanes will use airspace below FL 120 (12,000 feet MSL), the altitude at which FAA regulations require pressurization or oxygen equipment.¹ SATS operators may not be the only users of this airspace. In this section, we consider competitors to SATS for airspace below FL 120.

Airlines

Presently, airlines rarely use airspace below FL 120 except for arrivals and departures. Turbojet aircraft avoid this airspace for reasons of fuel economy. Figure 4-1 shows how rapidly optimum fuel burn per distance flown increases, and the the true airspeed (TAS) that yields the optimum burn decreases, when a regional jet transport, the Canadair CL600, operates at lower altitudes.

¹ While personal oxygen supply systems for small aircraft are available, their use is inconvenient, and it introduces complex safety issues. We do not consider this option for SATS.

Figure 4-1. Fuel Burn and Associated Airspeed For Canadair CL600 Regional Jet

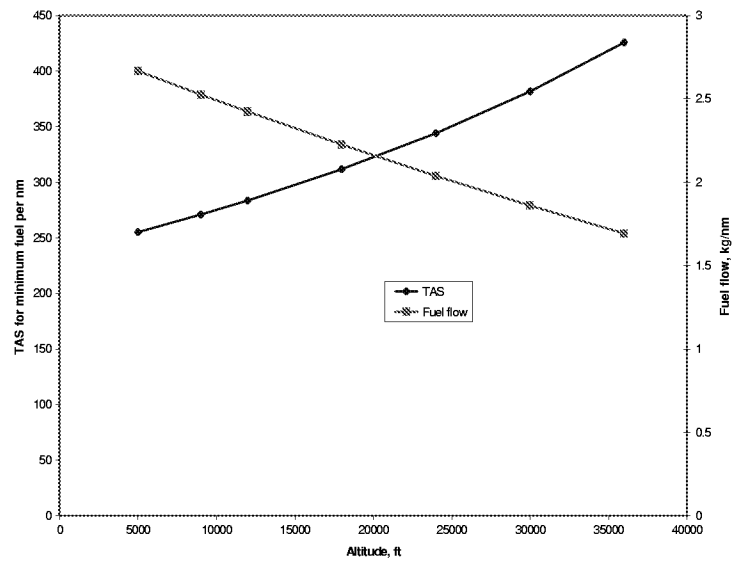


Figure 4-2 shows that turboprop aircraft do not experience the same degradation of fuel economy with decreasing altitude.

Figure 4-2. Fuel Burn and Associated Airspeed For Embraer E120 Turboprop

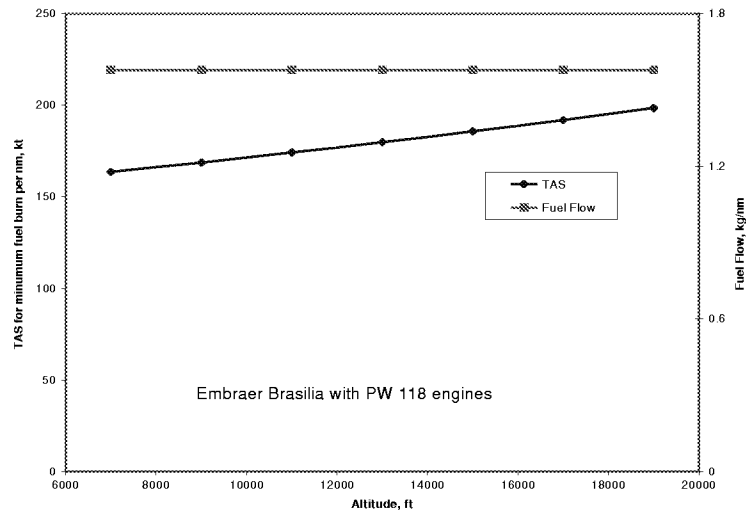
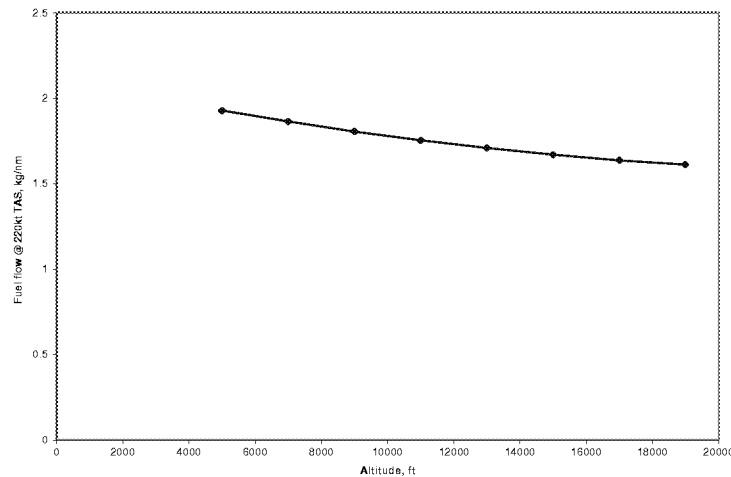


Figure 4-3 shows that fuel burn for a turboprop like the Embraer E120 does not increase rapidly with TAS.

Figure 4-3. Variation of Fuel Burn with TAS at FL 180, Embraer E120



In view of these facts, airlines flying turboprop aircraft have the option of operating at altitudes well below FL 100 without paying a great penalty in fuel economy, even when speed is not reduced.

There are reasons other than economy for airlines to avoid lower altitudes, such as increased turbulence and increased possibilities of encountering adverse weather requiring detours. Nevertheless, we believe that as the national airspace (NAS) becomes saturated, operators of turboprop equipment may decide to use altitudes where piston SATS airplanes fly. If the choice becomes a 30-minute delay for FL 180 and an immediate departure on FL 60, many turboprop airliner operators will choose the lower altitude.

Special Use Airspace

Significant parts of the airspace over the contiguous United States (CONUS) are reserved for special uses. This special use airspace (SUA) comprises military operations areas (MOA), restricted areas (RA), warning areas (WA), and prohibited areas (PAs). SATS traffic must respect these.

Nevertheless, the special characteristics of SATS airplanes may considerably reduce the effect of SUA on their operations. Single-engine and propeller-driven multi-engine SATS airplanes often can operate either below or above SUA. For example, there are 71 MOAs on IFR Enroute Low-Altitude Charts L-17 and L-18, which cover the south coast of the United States from west of Houston to east of Jacksonville. This region has many military installations, and thus many MOAs and RAs. Of the 71 MOAs, only four block all reasonable altitudes for propeller-driven SATS traffic.

Many SUAs do not operate all the time. For example, none of the four altitude-restrictive MOAs mentioned in the preceding paragraph operates continuously, and two of these never operate before 5 p.m. local time. Of 52 RAs on Charts L-17 and L-18, only 12 operate continuously and affect all propeller-SATS altitudes.

Moreover, many SUAs have relatively small areas. For example, restricted area R-3803A, one of the 12 continuously-operating SUAs on Charts L-17 and L-18 that obstructs all reasonable propeller-SATS altitudes, can be enclosed in a rectangle roughly 10 nm by 5 nm.

SATS operations will begin several years after 2001, when SUA may be revised and its area reduced. Also, the self-separating technology envisaged for SATS may interact automatically with SUA controllers to reduce to a minimum the effect of SUAs on SATS operations.

Nevertheless, in certain locations, great circle routes between SATS airports do cross continuously operating SUAs that affect all altitudes. The SUA near Edwards AFB, east of Los Angeles and that near Holloman AFB, are examples.

On balance, we believe that it is reasonable to neglect SUA in taking a first look at SATS traffic. A more detailed study, taking into account specific SATS separation technologies and the characteristics of specific SUAs, is desirable for more refined discussion. As a check on the reasonableness of neglecting SUA initially, the implementation of LMINET-SATS used in this study checks traffic through SUA near Edwards and Holloman Air Force Bases.

Mountains

Mountains would obstruct piston SATS traffic over significant portions of the western United States. Single-engine SATS airplanes cannot make flights on great circle routes between certain SATS airports in these regions. We have not adjusted SATS trajectories for mountains for two reasons. First, in many cases passes allow SATS traffic to operate with modest increases in distance. Second, the cases where terrain interferes with great-circle operations are between lightly populated areas and constitute relatively small fractions of SATS operations.

SATS AND ATM STAFFING

If SATS operations can be done under Visual Flight Rules (VFR), the effect of SATS on air traffic management will be reduced. SATS airplanes are light, so in addition to the VFR requirement, crosswind limitations should be considered. To get a preliminary indication of the fraction of the time that weather, including surface winds, will allow SATS VFR operations, we considered a trip from an airport in the New York area, MMU, to BED near Boston.

Our crosswind limitation was 15 knots. Although we know of no FAA or manufacturers' restriction on crosswind operations, light airplane makers typically demonstrate operations in no more than 15 knot crosswinds. Personal experience suggests that such winds pose a fairly significant challenge for a relatively inexperienced pilot.

MMU has two runways, as does BED. Using U. S. Weather Service (OASIS) data and taking EWR for MMU and BOS data for BED, we found that, for the calendar years 1981 through 1995, 90.7 percent of the time a SATS pilot would find MMU in VMC with acceptable crosswinds, and also would find BED in that state an hour later.

This example suggests that VFR SATS operations, while possible a large fraction of the time, probably are not sufficiently often available to suit the needs of business travelers. Missing or rescheduling a meeting one time out of ten is probably not acceptable to most business people. Thus, SATS operations supporting business travel must be able to operate in IMC. It also follows that business-related SATS activity will require ATM staffing capable of supporting it during IMC.

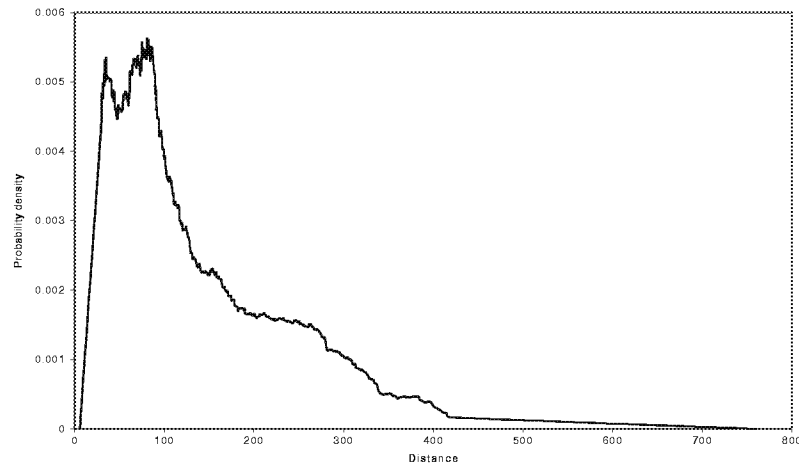
The burdens that SATS operations impose on the ATM system will vary with their tracks. An SATS flight departing IFR from an uncontrolled airport, flying a track that never enters airspace "owned" by a Terminal Radar Approach Control (TRACON), and landing at another uncontrolled airport presumably would require services only from the low-altitude sectors through which the track passed. If the track did pass through airspace controlled by a TRACON, that TRACON would service the flight. For example, a recent IFR flight of a Cessna 150 from Leesburg, Virginia, (JYO) to Bradley International Airport, Windsor Locks, Connecticut, (BDL) received services from seven different TRACONs and was controlled only briefly by Washington ARTCC, even though it never transited Class B airspace.

Light airplanes regularly operate under IFR. In addition to the analysis of this traffic described in Chapter 3, we examined ETMS data for April 8, 1996, for indications of the nature of present light-aircraft IFR flights to gain more information about the kinds of trips that SATS aircraft might take.

To have data for light aircraft only we considered IFR trips by Cessna 150, 152, 172, 177, 180, 182, 185, and 195 airplanes, together with IFR trips by Piper Cherokee (PA28) airplanes. We found ETMS records for 1,035 IFR flights between 0600 EDT and 2200 EDT on that date. Some of these had intersections, rather than airports, as destinations. We ignored these because they give no indications of intercity traffic. We also ignored round-robin flights with identical origin and destination airports for the same reason. Certain ETMS records appeared garbled, (e.g., an airport identifier with 9 characters) and we ignored these as well.

This left 889 flights. Figure 4-4 shows the distribution of the distances of these flights.

Figure 4-4. Distribution of Distances of 889 IFR Flights of Light Aircraft



The probability density of Figure 4-4 has a mode near 35 nm, and another near 85 nm. It is likely that the first mode largely represents training flights. The rapid decrease in frequency of flights beyond about 100 nm may reflect light airplanes pilots' preferences for flight legs taking no longer than 1 to 2 hours.

The very small numbers of flights for distances greater than 400 nm is consistent with confronting IFR endurance requirements with light aircraft fuel capacities. Meeting the requirement for sufficient fuel to fly to the destination, thence to an alternate, and land with 45 minutes of fuel remaining, generally would limit light aircraft to legs of about that length. Favorable winds, light loads, and pilot endurance may, of course, enable longer flights.

DEFINITION AND OPERATION OF LMINET-SATS

LMINET-SATS provides an addition to LMINET that tracks SATS operations, and their interactions with LMINET sectors and TRACONS. It provides 2,865 airports.

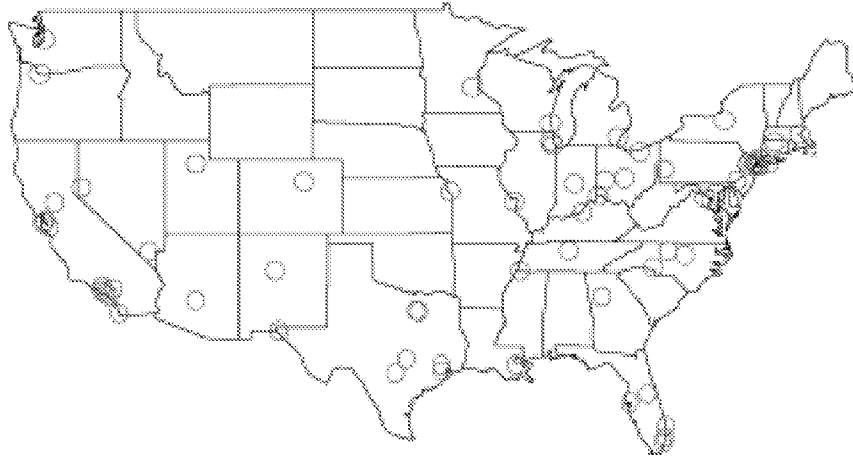
Input to LMINET-SATS is a list of SATS flights between SATS airports, giving origin, destination, and starting time for each. Outputs are the number of SATS flights in each LMINET geographic sector, and in each LMINET airport's TRACON, epoch by epoch. These traffic data may be added to LMINET traffic data, to analyze SATS effects on the NAS.

This section gives the considerations that led to the definition of LMINET-SATS, describes its operations, and gives some example outputs.

Considerations for Adding a SATS Underlayer to LMINET

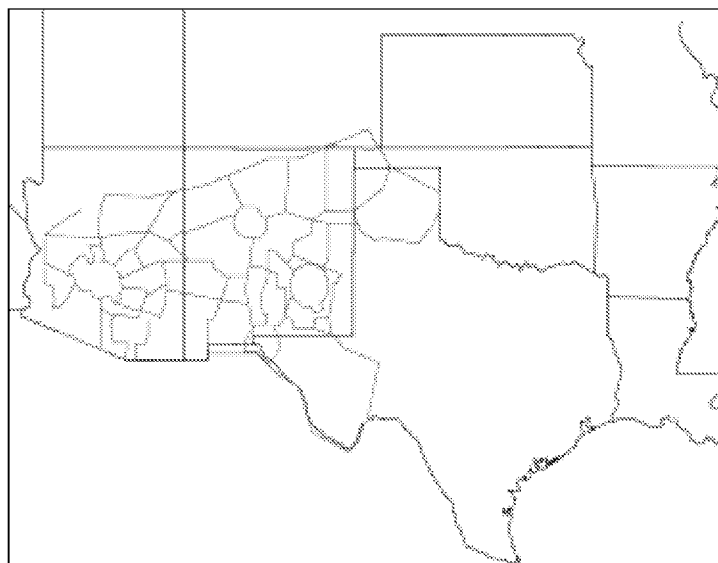
Generally, ARTCC controllers do not handle IFR traffic below FL 100 and within 30 nm of a Class A airport. Rather, controllers in the airport's TRACON will direct that traffic. In some parts of the NAS, significant fractions of the airspace are within 30 nm of a Class A airport. Figure 4-5 shows the regions within 30 nm of the 64 LMINET airports.

Figure 4-5. Thirty nm Zones around LMINET Airports



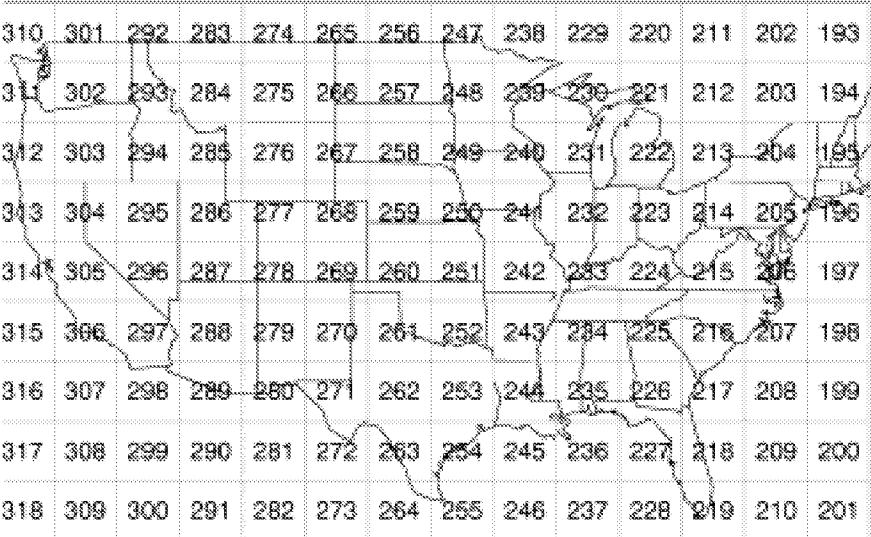
The FAA's low-altitude sectors clearly recognize the presence of TRACON airspace. TRACON airspace for Albuquerque (ABQ), Phoenix (PHX), El Paso (ELP), Chisum (CME), and Tucson (TUS) is clearly visible in Figure 4-6, which diagrams the low-altitude sectors for the Albuquerque ARTCC.

Figure 4-6. Low-Altitude Sectors for Albuquerque Air Route Traffic Control Center



Users can define any partition of the NAS by a collection of points, and use the result as en-route sectors in LMINET. All LMINET studies to date have considered NAS operations many years in the future. Geographical sectors, rather than the present FAA sectors, were used in these studies because the studies were specifically directed not to constrain operations by the present airway and sector structures. Sector results from these studies highlight geographic regions of heavy traffic, when traffic operates on optimal routes. Figure 4-7 shows a plan view of basic geographic enroute sectors used in recent LMINET studies. In most of these studies, heavily traveled basic sectors were viewed as divided into as many as nine subsectors.

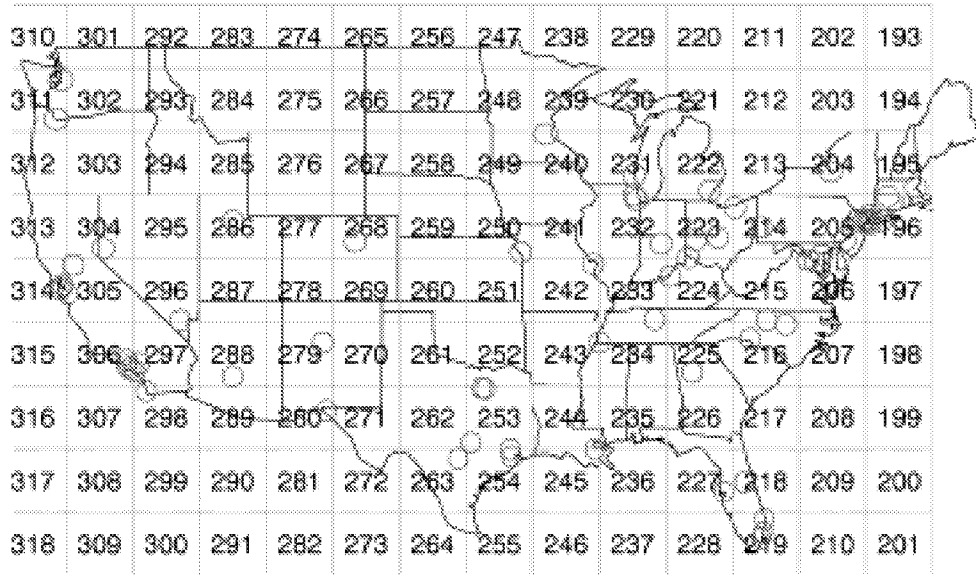
Figure 4-7. Geographic Enroute Sectors



Because fully developed SATS will happen more than a decade in the future, we believe that the SATS study also should use geographical sectors for air carrier traffic, at least initially. This will give consistency with previous studies, and will avoid constraining SATS operations by the airways and enroute sectors of today's NAS.

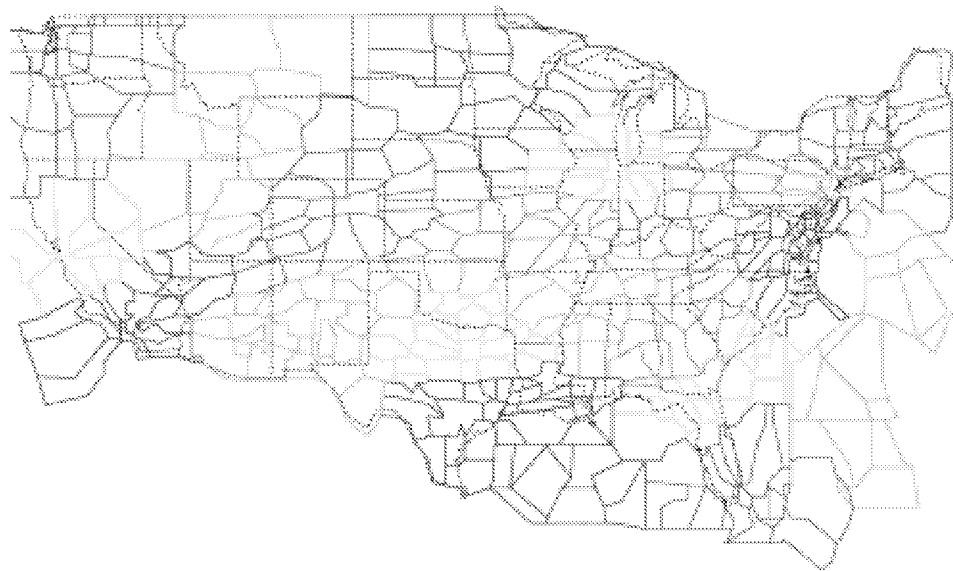
Light-aircraft SATS operations under IFR are likely to affect TRACONS, in addition to ARTCC sectors, because they typically will operate below FL 100. Accordingly, we intend to use the enroute sector structure of Figure 4-8 for light-aircraft SATS operations.

Figure 4-8. Enroute Sector Structure For Light-Aircraft SATS Operations



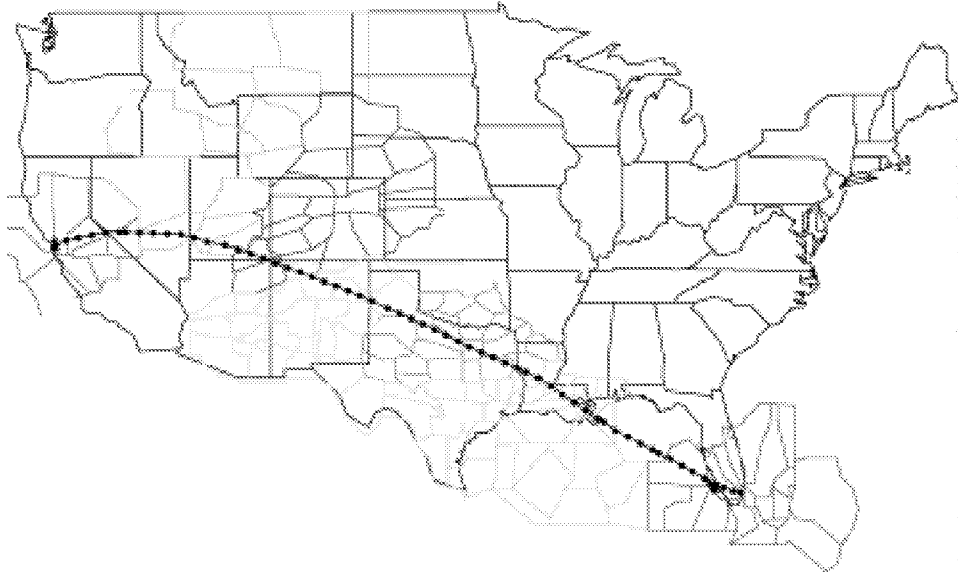
If the effects of SATS on workloads in the present NAS are desired, we will use the FAA’s high-altitude sectors, shown in Figure 4-9, for air carrier traffic and turbine SATS traffic. Figure 4-6 is an example of the FAA’s low-altitude sectors that we will use for low-altitude SATS traffic.

Figure 4-9. FAA High-Altitude Sectors



FAA sectors are closely, and sometimes quite narrowly, linked to present J- and V- air route structures. To use the FAA sectors effectively, we will take as LMINET air carrier and SATS turbine trajectories not the wind routes used in previous studies, but representative ETMS trajectories. Figure 4-10 shows an example.

Figure 4-10. Example Trajectory



Light SATS traffic, however, appears likely to relate differently to the air route structure. Light SATS trips will be short, usually not more than 300 nm, and they will take place below FL 120. Presently, we are inclined to send light SATS traffic on great circle routes, perhaps avoiding TRACON airspace enroute.

Under IFR, a light-aircraft SATS flight will impose load on the sectors through which it passes, either geographic or FAA, and also on the TRACONs of each LMINET airport to which the flight gets as close as 30 nm. In some areas, notably the mid-Atlantic coastal region, flights may be handled entirely by TRACONs. We will track SATS light-aircraft traffic separately from other TRACON traffic so that analyses may consider this traffic to be handled by separate TRACON stations.

Following is a brief description of airports in LMINET-SATS, the extension of LMINET to model SATS operations.

- ◆ LMINET-SATS has two airport classes, “major” and “SATS.” The major airports are the 64 LMINET airports. The SATS airports make up a set of about 800 other airports. The SATS airports generally will have at least one hard-surfaced runway not less than 2,000 feet long.
- ◆ Major airports’ capacity models are the present LMINET capacity models. Air carrier operations at these airports are modeled as in the present LMINET. Because the purpose of our study is to model SATS as relief to major airports, SATS operations with piston aircraft *do not* involve major airports. (Of course, SATS-to-major airport and major-airport-to-SATS operations in light aircraft are possible, and they could be modeled if such operations did not violate the light SATS spirit.)

- ◆ SATS operations with turbine equipment may involve major airports.
- ◆ SATS operations in IFR involve TRACONS when the route is within 30 nm of a major airport. We make this stipulation because the FAA presently does ATM this way.
- ◆ SATS airports capacity models are adapted from present LMINET airport models. There is no reservoir of ready-to-depart aircraft because SATS operations are assumed to use on-base resources. Taxi-out, departure runway, taxi-in, and arrival runway are modeled as in LMINET.

Following is a list of services required by SATS operations:

- ◆ Piston (four-place, single-engine piston) SATS operations
 - SATS airport to SATS airport
 - Taxi-out;
 - Departure runway;
 - If departure airport is within 30 nm of a major airport, departure TRACON;
 - Low-altitude ARTCC subsectors where the track passes through;
 - If track passes within 30 nm of a major airport, the airport's arrival TRACON;
 - Arrival runway;
 - Taxi-in.
- ◆ Turbine SATS operations
 - SATS airport to SATS airport
 - Taxi-out;
 - Departure runway;
 - If departure airport is within 30 nm of a major airport, departure TRACON;
 - High-altitude ARTCC subsectors where the track passes through;
 - If arrival airport is within 30 nm of a major airport, arrival TRACON;

-
- Arrival runway;
 - Taxi-in.
 - SATS airport to major airport
 - Taxi-out;
 - Departure runway;
 - If departure airport is within 30 nm of a major airport, departure TRACON;
 - High-altitude ARTCC subsectors where the track passes through;
 - Arrival TRACON;
 - Arrival runway;
 - Taxi-in.
 - Major airport to major airport
 - Taxi-out;
 - Departure runway;
 - Departure TRACON;
 - High-altitude sectors where the track passes through;
 - Arrival TRACON;
 - Arrival runway;
 - Taxi-in.

SATS airports

We developed a set of SATS airports in this way: The FAA's Terminal Area Forecast (TAF) treats 3,412 airports and TRACONs. These include more than 400 airports receiving FAA and contract tower and radar service, and more than 3,000 other airports in the National Integrated Airport Plan. The airports are all public use airports, with at least one paved runway.

Not all the TAF airports are in the continental United States; however, and some of the airports listed, such as Andrews Air Force Base (ABW), are exclusively military facilities not likely to become available for SATS. Deleting the TRACONs, the exclusively military airports, and the 64 LMINET airports left a set of

3, 015 airports. We chose this collection as the set of SATS airports. Their locations are shown in Figure 4-11.

Figure 4-11. SATS Airports



Clearly, the SATS airports are quite widely distributed across the contiguous United States.

LMINET-SATS Operations

LMINET-SATS input is a file of demand for SATS flights. It is a flat ASCII file, giving a set of {epoch², origin, destination, number of flights} quadruples. For example, a very short input file would be

```
{ {0, YIP, GAI, 1}, {0, FWA, DPA, 3}, {3, BED, LDJ,1}, {2, SGH, GAI, 1} }
```

That file calls for one flight from Willow Run Airport near Detroit to Montgomery County Airport in suburban Washington, D. C., and one flight from Fort Wayne, Indiana, to DuPage, Illinois, a western suburb of Chicago in epoch 0, followed by a flight from Springfield, Ohio, to Montgomery County Airport in epoch 2, and a flight from Hanscomb Field, near Boston, to Linden, New Jersey, near New York City, in epoch 3³.

Up to 27,500 SATS departures may be scheduled in each epoch. For each of these, LMINET-SATS generates the set of LMINET sectors through which the flight would pass, and the epochs during which the flight will occupy them.

LMINET-SATS also generates the set of LMINET airports for which the flight passes within 30 nm, and the epoch of arrival in each 30 nm ring. We believe these data are important because SATS flights must at least have the option of operating under IFR if they are to be sufficiently reliable for business travel and because the

² LMINET operates on epochs, which may be 1 hour or 1/2 hour long. Presently 1-hour epochs are used.

³ In the operating LMINET, the airport codes are replaced by integer identifying numbers.

FAA controls IFR traffic within the Mode C Veil, not via ARTCC sectors, but via the TRACONs of the airports involved.

Presently LMINET-SATS trajectories for propeller-driven SATS airplanes are great circles. We assume that single-engine SATS airplanes cruise at 160 kt GS, and that piston-driven multi-engine SATS airplanes cruise at 190 kt GS.

We believe that the assumption of great circle routes for propeller-SATS airplanes is not particularly restrictive. Their trips generally are less than 320 nm, and so are not likely to be long enough for optimization for varying wind to have significant effects. (Please see the sections on “Special Use Airspace” and “Mountains” for discussions of SUA and terrain effects.)

The assumption of zero wind is somewhat restrictive. Winds aloft often reach 20 percent of prop-SATS cruising speed, and in a subsequent report we will extend the LMINET winds-aloft model to the altitudes at which prop-SATS flights will operate.

For an example of the operation of LMINET-SATS, consider the flight from YIP to GAI starting in epoch 0. The first NAS facility to be affected is the DTW TRACON, in epoch 0. LMINET geographic sector 223, and the CLE TRACON, also handle the flight in epoch 0.

The flight arrives at sector 214, passes through the PIT TRACON, and re-enters sector 214, in epoch 1. We believe that the two entries into sector 214 do not represent double counting, because there would be a handoff from sector 214 to the PIT TRACON, and another from that TRACON to sector 214.

In epoch 2, the flight continues in sector 214, then enters sector 205, and, finally, enters airspace of the IAD TRACON. We believe it is reasonable to count the slow-moving prop-SATS traffic as affecting an LMINET sector during each epoch in which it occupies the sector. Since a prop-SATS flight would occupy the Mode C Veil of a given airport no longer than 22.6 minutes, even if a prop-SATS flight is in a TRACON during two epochs, we count it only in the first one.

RESULTS

In this section we discuss results of operating LMINET and the underlayer, LMINET-SATS.

An initial exercise

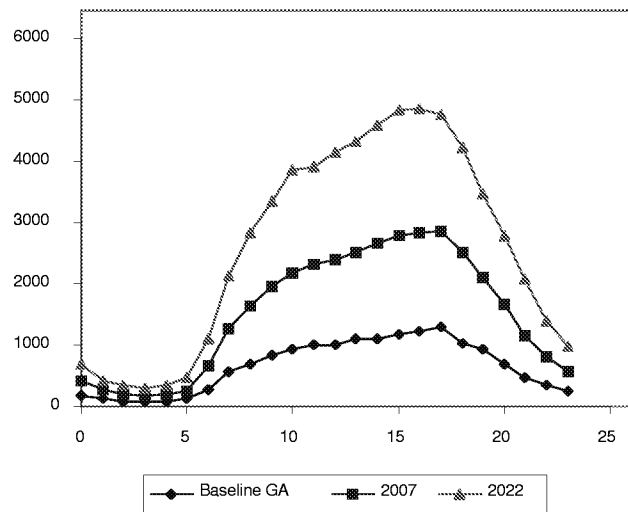
As an initial exercise of the SATS underlayer of LMINET, we considered four demand cases. Two of these were for SATS delivering 1 percent of RPM demand, in 2007 and 2022. The final two cases were for SATS delivering the difference between RPM demand and the RPM delivered by air carriers, enjoying the benefits of NASA ATM technology and of new hubs, increased point-to-point routes, schedule

smoothing, and night in 2007 and 2022. Chapter 3 explains how we developed these demand schedules.

WHEN SATS DELIVERS 1 PERCENT OF RPM DEMAND

Figure 4-12 shows the total number of SATS departures required to deliver 1 percent of demanded RPM in 2007 and 2022.

Figure 4-12. Hourly SATS Departures Required to Meet 1 Percent of RPM Demand



These operations would substantially increase operations at several SATS airports. Nevertheless, as shown by the examples of Figures 4-13 and 4-14, for many airports the increases appear to be well within capacity. VNY and MMU both have four runways, one with ILS. VNY has a continuously operating tower; MMU’s tower operates from 0645 to 2230, which covers all the busy periods shown in Figure 4-14.

Figure 4-13. Piston ILS Arrivals at Van Nuys, California

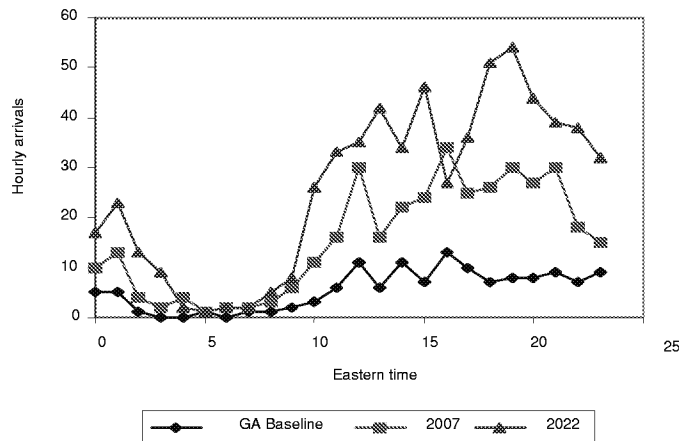
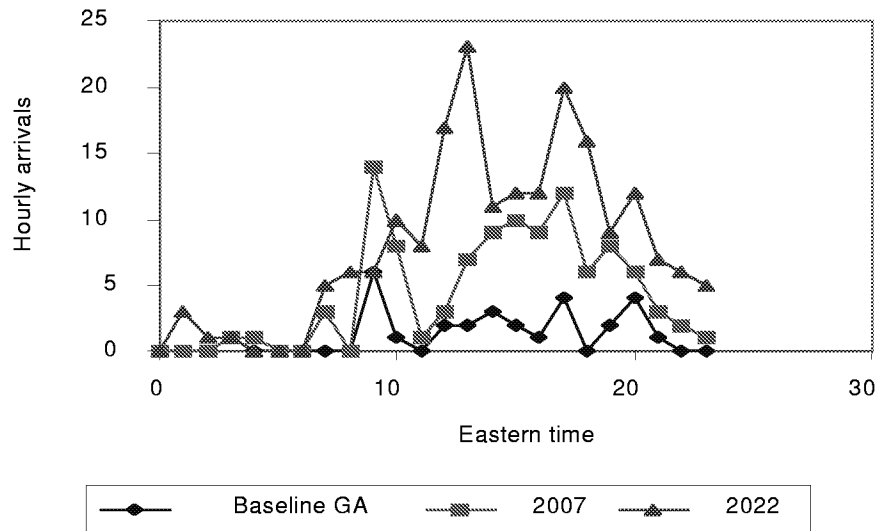


Figure 4-14. Piston ILS Arrivals at Morristown, New Jersey



Now we explore the effects of SATS delivering 1 percent of demanded RPM on enroute sectors and TRACONS. We consider enroute sectors first.

Present FAA standards restrict the number of aircraft in a subsector to values ranging from 15 to 21. Present subsectors often conform closely to present airways, and their boundaries may be changed. So, rather than treat any specific present sectors, we will consider what sorts of traffic densities might be accommodated in the airspace above geographic regions, with present ATM methods. The present LMINET-SATS results give data for sectors roughly 120 nautical miles on a side.

Piston-driven SATS aircraft will not be pressurized. Accordingly, they will not operate at altitudes above 12,000 feet MSL. Much of the CONUS has ground levels at or above 1,000 feet MSL. Prudent cruising altitudes probably will not be less than about 3,000 feet AGL, to avoid obstacles and to give reasonable opportunity for a successful forced landing. Thus the available range of enroute altitudes for piston SATS airplanes appears to range from 4,000 feet to 12,000 feet MSL.

With present conventions, there would be nine IFR altitudes in that range, five westbound and four eastbound. Many present ARTCC subsectors that are 900 to 1,000 feet thick, so it seems reasonable to assume that each of the available altitudes could belong to a distinct sector.

Dividing a 120 nm by 120 nm square into geographic subregions could be done in many ways; nevertheless, achieving more than about four subregions seems questionable. If the division were divided into equal subsquares, each would be 60 nm on a side. Propeller SATS aircraft would transit such regions in about 22 minutes.

It seems likely that much shorter times-in-sector would make coordination among sector controllers difficult.

Division into subregions parallel to one pair of the original region's sides might be effective in places where the SATS traffic was all headed in much the same pair of reciprocal directions. Taking these long, narrow corridor subregions less than about 30 nm wide makes heavy restrictions on the set of trajectories that could be accommodated. Propeller SATS aircraft typically would spend about 40 minutes in a corridor sector.

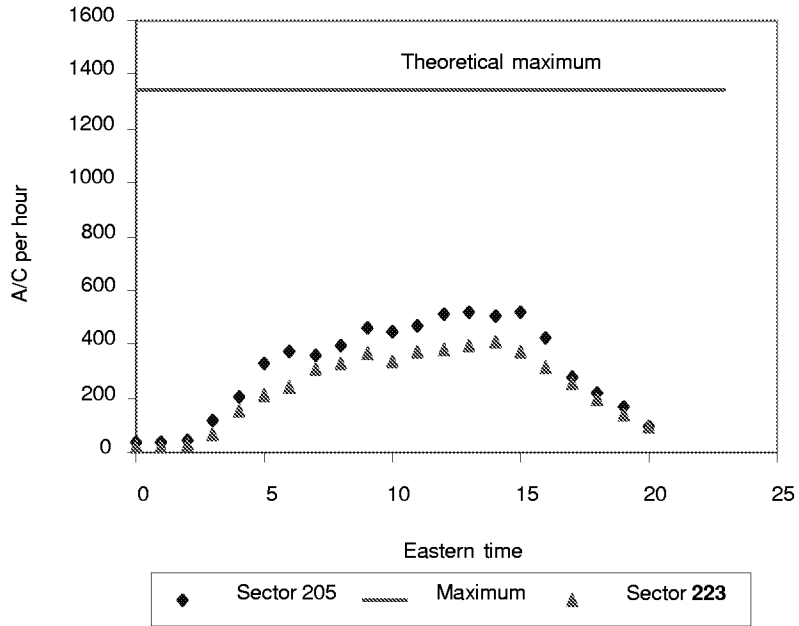
We conclude that present ATM methods are unlikely to result in more than about 36 independent subsectors in each 120 nm by 120 nm region.

If interarrival times of aircraft at a sector follow a Poisson distribution—which ETMS data indicate is the case for the present FAA sectors⁴—and spend 20 minutes in the sector, then the number of aircraft in a sector at one time also will have a Poisson distribution, with mean equal to one-third the hourly arrival rate. To keep the number of aircraft in a sector at or below 18 with 95 percent confidence, the hourly arrival rate should not exceed 37.33. If the 120 nm by 120 nm LMINET sectors are divided into four subregions geographically, and into nine altitude layers, the hourly arrival rate to the LMINET sector should not exceed $37.33 \times 36 = 1344$. (That rate is an upper bound—probably a generous one—on a practical arrival rate. The FAA is not likely to put 36 controllers to work on eight thousand feet of altitude over one 120 nm by 120 nm geographic region!)

Figure 4-15 shows hourly demands for certain LMINET sectors approach one-third of the theoretical maximum, when SATS aircraft deliver 1 percent of the RPM demanded in 2007. The figure also shows only SATS traffic, but there will be other demands for ATM services. As we noted above, saturation of enroute sectors in Class A airspace (above 18,000 feet) may cause operators of turboprop transports to use lower altitudes.

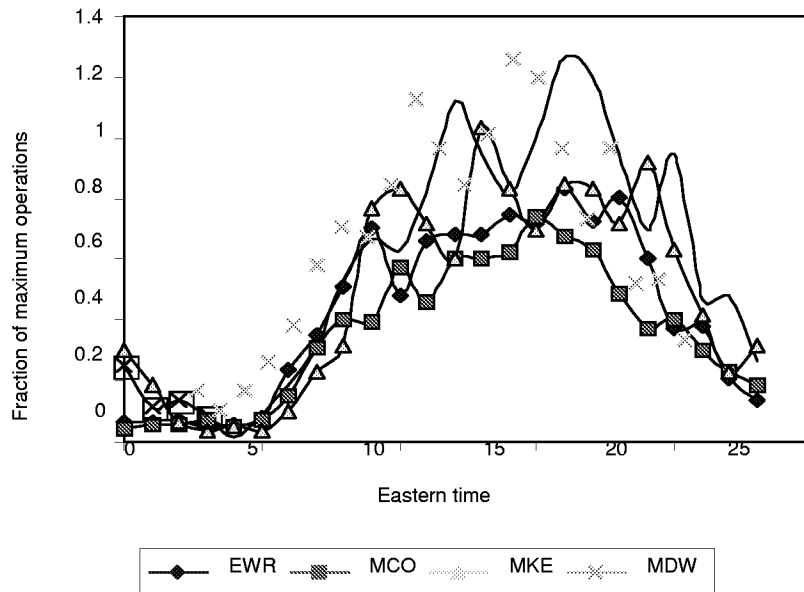
⁴ Lee, D. A. et al., "Technical and Economic Analysis of Air Transportation Management Issues Related to Free Flight," Logistics Management Institute Report NS501T1, McLean, VA, February 1997.

Figure 4-15. Hourly Demand For Busy Sectors, 2007



The burden imposed by SATS aircraft on certain TRACONs also is significant. When an IFR flight is within the mode C veil of an airport with Class B airspace, that airport's TRACON handles the flight. We computed SATS TRACON demands as a fraction of maximum hourly operations for several airports, taking the LMINET capacity for an airport as a measure of that maximum. Figure 4-16 shows the results.

Figure 4-16. SATS TRACON Demands, 2007



Figures 4-15 and 4-16 strongly suggest that delivering 1 percent of demanded RPM by SATS in 2007 would pose significant, but probably not impossible, demands on air traffic management by present methods.

Now we consider when SATS delivers 1 percent of demand in 2022. Figures 4-17 and 4-18 update Figures 4-15 and 4-16, respectively, to that year.

Figure 4-17. Hourly Demand For Busy Sectors, 2022

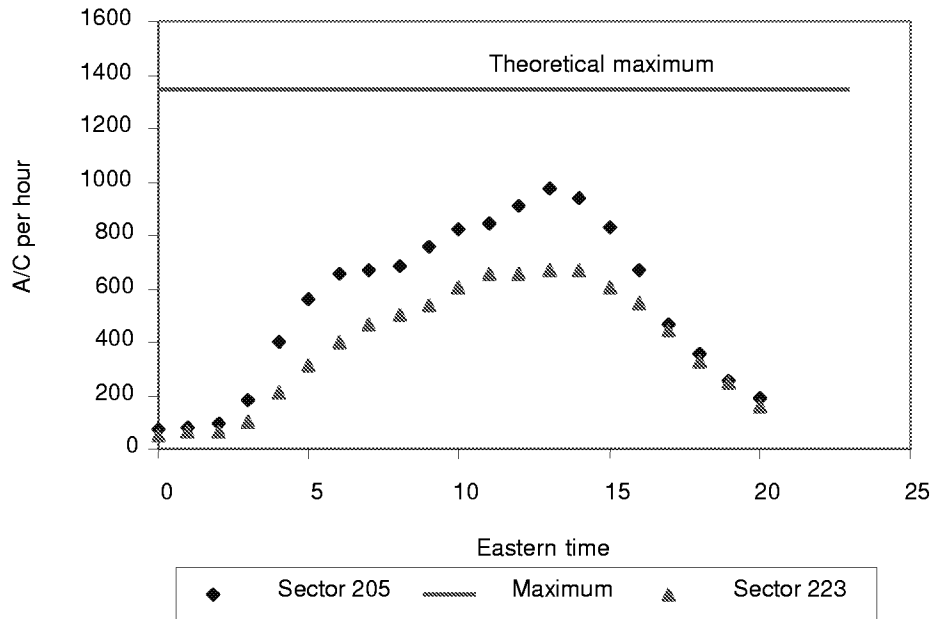
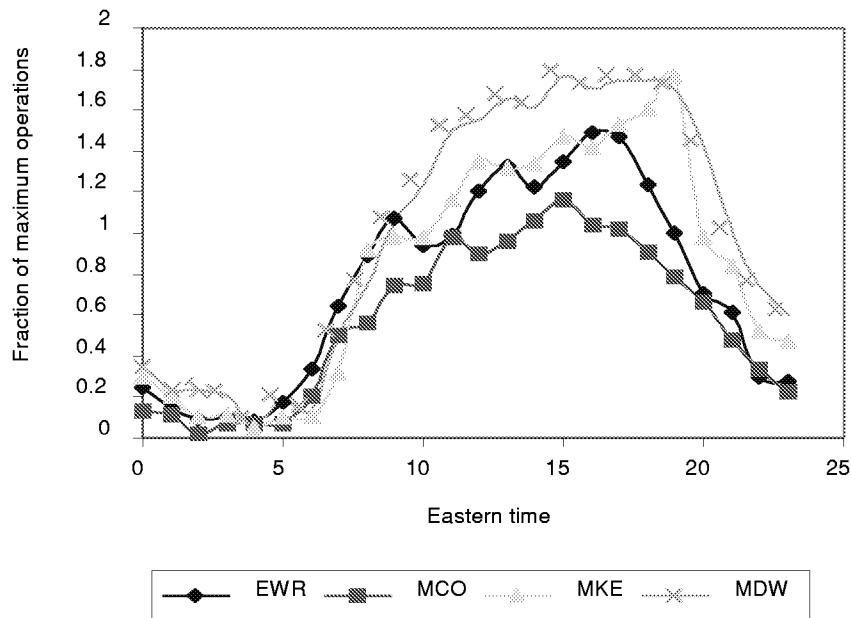


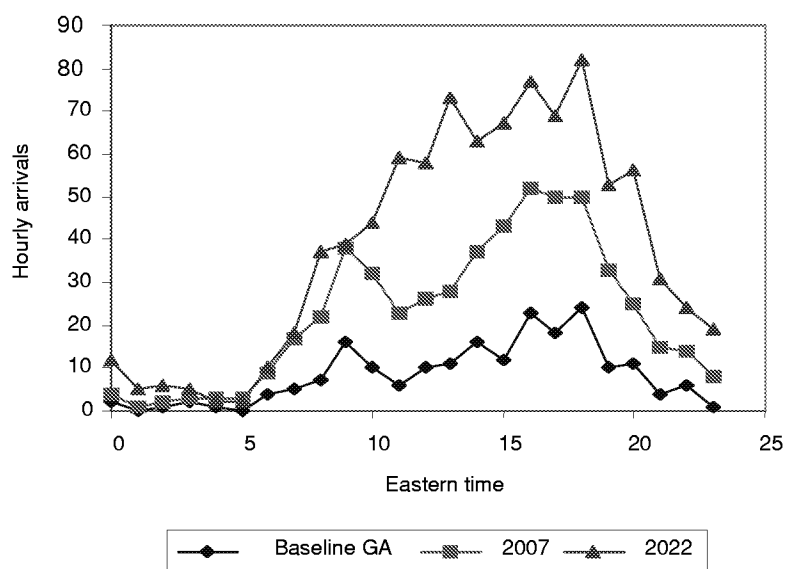
Figure 4-18. SATS TRACON Demands, 2022



At the 2022 levels, the demands for both sector and TRACON services made by SATS aircraft meeting 1 percent of RPM demand are great enough to raise questions about satisfying them with present ATM methods. Sector effects reach 70 percent of the theoretical maximum, and TRACON effects substantially exceed the demands made by arriving and departing flights when certain airports are working to capacity.

We also considered arrivals to SATS airports close to major terminals. Figure 4-19 shows hourly IFR arrivals to the 14 SATS airports within 30 nm of EWR (TEB, MMU, CDW, LDJ, 39N, N52, N07, 6N4, N51, 4N1, 47N, 3N6, JRB, and 6N5).

Figure 4-19. Hourly Piston-SATS Arrivals to SATS Airports Near EWR

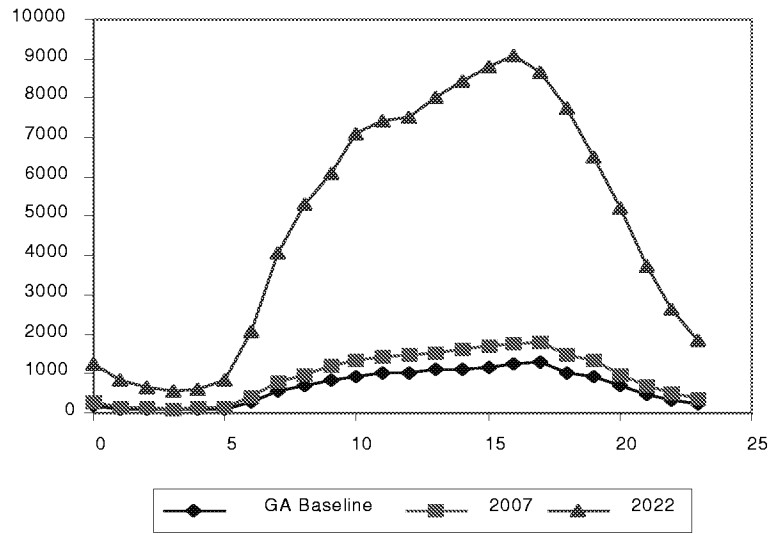


These arrivals may be more burdensome to the EWR TRACON than SATS flights that only transition TRACON airspace during cruise.

Effects of Improved Strategies

What are the effects of ATM when SATS delivers the difference between the RPM that travelers would consume absent any constraints by carriers' interests or NAS properties? What could be delivered if economically motivated carriers use improved strategies (e.g., new hubs, more direct flights, schedule smoothing, and night flights) in a NAS if certain NASA decision-support tools for ATM (e.g., TMA, MCTMA, A/PFAST, SMA/SMS, T-NASA, AVOSS, ROTO, DROM, and SVS) are fully implemented? Figure 4-20 shows the overall possible level of operations.

Figure 4-20. SATS Operations to Supply RPM Deficit



In 2007, the RPM deficit is small. SATS needs to provide even less than the 1 percent of RPM considered earlier. But in 2022, many more SATS operations are required.

All traffic measures considered in the 1 percent cases are greatly increased for 2022. Figure 4-21 shows examples of arrivals to VNY. The peak level of 120 hourly arrivals would be difficult to sustain with VNY’s present two runways.

Figure 4-21. Piston-SATS Arrivals to VNY, Deficit Case

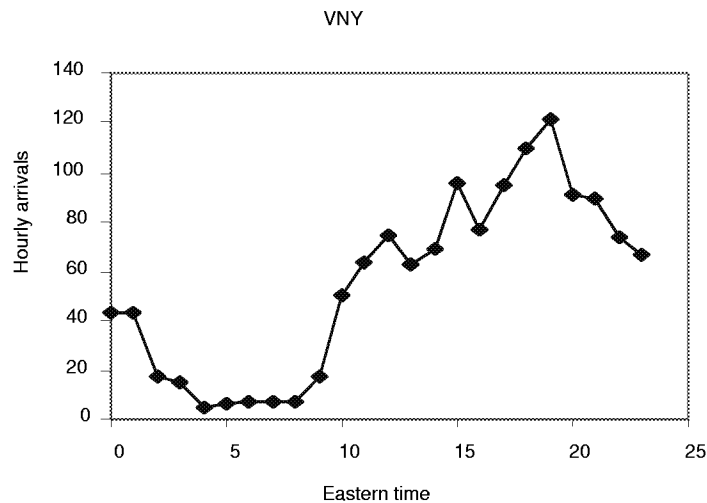
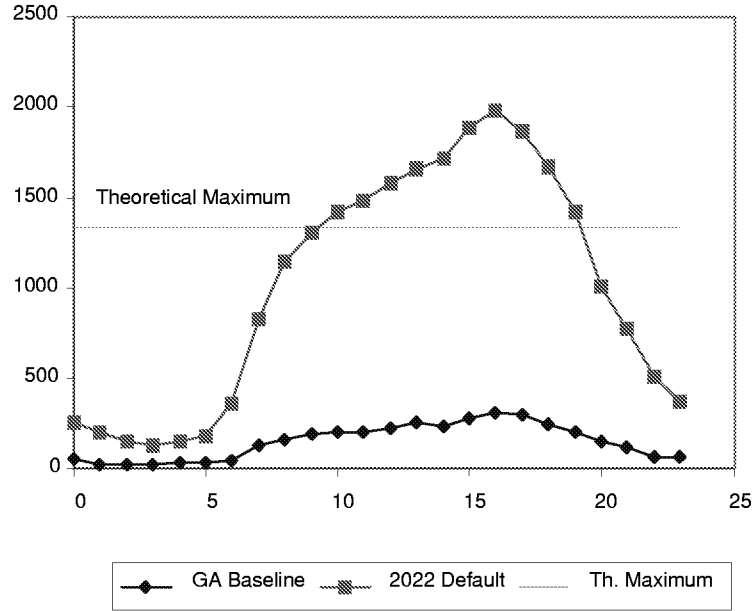


Figure 4-22 compares piston-SATS arrivals to Sector 205 when SATS makes up the deficit between RPM supplied by profit-motivated carriers using the NAS im-

proved by NASA tools, and also using improved carrier strategies, and the RPM forecast of the FAA TAF.

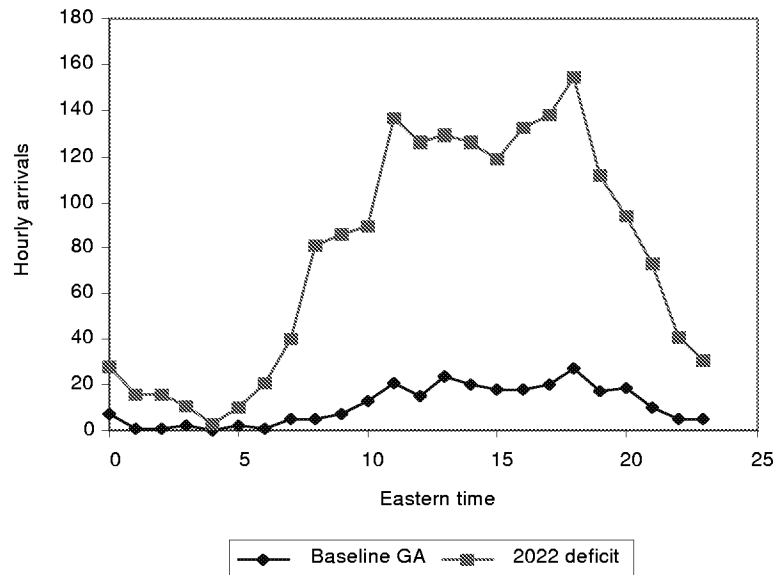
Figure 4-22. Arrivals to Sector 205



The highest demand levels would be difficult to sustain with present ATM methods.

Figure 4-23 shows hourly demand for piston-SATS arrivals at the 14 airports (other than major airports) located within 30 nm of EWR.

Figure 4-23. Arrivals To SATS Airports Near EWR, Deficit Case



Conclusions

In view of these early results on the demands that piston-SATS traffic would make on the ATM system, we make the following conclusions:

- ◆ SATS might deliver economically significant levels of RPM in 2007, while still supported by present ATM methods. The levels of traffic would not change materially the total RPM delivered by the air transport system.
- ◆ New ATM methods almost certainly would be required for SATS to deliver a significant fraction of total RPM provided by the air transport system in 2022. Some facilities, such as runways at certain SATS airports, might be taxed beyond their capacities when SATS functions at such a level.

Chapter 5

Summary and Future Work

The models presented in this report are powerful tools policy decision makers can use for air traffic system planning, especially in SATS planning. The models help predict SATS demand for airports and airspace. They are flexible, parameterized, easy-to-use tools to predict SATS demand in different scenarios, as shown by our case studies.

Readers should be aware that the figures we present in this report are not forecasts; they are the results of “what-if” studies to demonstrate the use of our models. The models, albeit developed with empirical data fitting and flexibility to change the parameters, are not the forecast models. They are “what-if” analysis tools. Our models can predict SATS demand based on the assumed scenarios. The models are constructed for easy link to any SATS demand forecast models, which may come from different sources.

In light of the current model development, our future emphasis will be estimation of the SATS demand curve, which will quantify the SATS demand for a given set of socioeconomic parameters, and a set of SATS performance and cost parameters. With completed SATS-FDM and LMINET-SATS for the SATS airspace demand, our future work should be the SATS demand model on a higher aggregate level, dealt with by SATS-ADM. Specifically, we need to develop a quantitative model of SATS operations for each aircraft type for each airport.

After we construct the SATS demand curve, we can use the model to analyze the effect of SATS on demography and economy in the area surrounding an airport. On another hand, SATS will have an impact on demography and economy in the area surrounding an airport. This will require a feedback loop in analyzing SATS demand and demography and economy. With the closed loop, we will complete the SATS demand model development.

The model will assume that air travels are induced economic activities that must satisfy basic economic laws. Predicted travel is the point where the demand curve and the supply curve meet. Generally, the mathematical model takes the following form:

$$T = f(\textit{socioeconomic parameters, cost of travel parameters}), \quad [\text{Eq. 5-1}]$$

where T is the measure of travel such as TPM defined in Chapter 2, for a city pair, for the total travel out of a city, or the total travel in a region such as the United States. A commercial air traffic example is the Air Carrier Investment Model (ACIM) in the Aviation System Analysis Capacity (ASAC) model suite. In

ACIM, T is the total U.S. RPM; the socioeconomic parameters are population, per capita income, and unemployment rate; the cost of travel is in revenue per seat mile (RSM), which depends on numerous costs for labor, material, maintenance, and acquisition, plus others; and competition in the marketplace measured in market share and the Herfindahl index.

Typically, to facilitate the parameter estimation, a linear model is assumed, although the products of variables frequently are included. If the model takes a log-linear form, then the parameters estimated are the elasticities (e.g., traffic will grow 2 percent for each 1 percent of per capita income growth if the elasticity of per capita income is 2.0, assuming all other factors hold constant).

After model parameters, or, more likely, elasticities, are estimated, we can analyze many what-if scenarios using various socioeconomic and cost parameters. This methodology has been successfully employed to assess the effect of traffic on air carrier business strategies and ATM technologies ([1,2]. Historical data are required to construct such a model. For example, the Forms 41 data from the Department of Transportation, 1985 through 1994, at the largest 85 U.S. domestic airports by all airlines are used to estimate the parameters in ACIM. No historical data for SATS exist. If we used models such as ACIM for forecasting SATS demand by varying the input variables, we would implicitly assume that the model structure will be intact even with different sets of input and output variables. The SATS economic demand model must be different, in both mathematical form and the values of elasticities, because it is a different mode of transportation. It is not possible to borrow one model in another mode of transportation, or to use an old model after the industry experiences structural change. An example is exponential growth of commercial air traffic offered by air carriers and the gradual decline of GA traffic in the past two decades in the United States.

It is not plausible to use historical GA data to build a SATS traffic demand model because the two are different travel options. The proposed SATS will be more cost-effective to acquire and operate, faster and easier to operate, and require less pilot training.

Building such a model will be a challenging, creative task. A set of modeling principles will help in our modeling:

- ◆ The model must be based on sound economic principles.
- ◆ The model must use the available data fully.
- ◆ The model must be as comprehensive as possible to consider potential SATS demand scenarios, which will consider diverted demand from commercial travel, latent demand, and mode selection of all transportation means including ground-based.
- ◆ The model is best constructed by linking a set of component models.

- ◆ If one component model is unavailable, the hooks for its later connection and appropriate default values must be provided. Furthermore, the modeler must identify the mechanism and the data needed to construct the missing component model.
- ◆ To capture the essence of SATS demand, the model should be as simple as possible. The model should have as few adjustable parameters as possible because each adjustable parameter in the model represents a subjective input and a source of uncertainty. This principle is not inconsistent with the need for a comprehensive model. While the need for a comprehensive model includes all demand sources, the need for a simple model gives priority to simplicity over complexity in mathematical equations, especially in light of the uncertainties of SATS demand functions.
- ◆ Adjustable parameters in the model must be interpreted easily. Ideally, they should serve as the hooks of the connection so that running the model involves picking values in a set of well understood parameters, which can be further determined by component models.

References

- [1] Peter F. Kostiuk, Eric M. Gaier, and Dou Long, “The Economic Impacts of Air Traffic Congestion,” *Air Traffic Control Quarterly*, Vol. 7(2), 1999, pp. 123–145.
- [2] Logistics Management Institute, *A Method for Evaluating Air Carrier Operational Strategies and Forecasting Air Traffic with Flight Delay*, Dou Long, et al., October 1999.
- [3] NASA, *A Method for Making Cross-Comparable Estimates of the Benefits of Decision Support Technologies for Air Traffic Management*, NASA Contractor Report 208455, David A. Lee, Dou Long, Melvin R. Etheridge, Joana R. Plugge, Jesse P. Johnson, and Peter F. Kostiuk, 1998.
- [4] NASA, *Modeling Air Traffic Management Technologies with a Queuing Network Model of the National Airspace System*, NASA Contractor Report 208988, Dou Long, David A. Lee, Jesse P. Johnson, Eric M. Gaier, and Peter F. Kostiuk, 1998.
- [5] NASA, *A Method for Forecasting the Commercial Air Traffic Schedule in the Future*, NASA Contractor Report 208987, Dou Long, David A. Lee, Eric M. Gaier, Jesse P. Johnson, Peter F. Kostiuk, 1998.
- [6] NASA, Aviation System Capacity Program, Advanced Air Transportation Technologies, *ATM Definition, Volume 1, Current and Future Operational Concepts for the National Airspace System, Volume 2, Coverage of Future National Airspace Operational Requirement*, October 21, 1997.
- [7] NASA, *National General Aviation Roadmap—Definition Document for a Small Aircraft Transportation System Concept*, Bruce Holmes, NASA General Aviation Program Office, Langley Research Center, March 4, 1999.
- [8] NASA, *Small Aircraft Transport System—Strawman Features & Capabilities*, Office of Aeronautics and Space Transportation Technology
- [9] Federal Aviation Administration, *National Plan of Integrated Airport Systems (1998–2002) (NPIAS)*, March 1999, Washington, D.C.
- [10] Federal Aviation Administration, *General Aviation and Air Taxi Activity Survey (GAATA)*, Statistics and Forecast Branch, Planning Analysis Division, Office of Aviation Policy and Plans, March 1999, Washington, D.C.

-
- [11] Federal Aviation Administration, *National Airspace System Architecture*, Office of System Architecture and Investment Analysis (ASD-1), 800 Independence Avenue, SW, Washington, D.C., December 1997.
- [12] Federal Aviation Administration, *FAA Long-Range Aviation Forecasts Fiscal Years 2010, 2015, and 2020*, Office of Aviation Policy and Plans, 800 Independence Avenue, SW, Washington, D.C., June 1998.
- [13] Department of Transportation, *FAA Aerospace Forecasts—Fiscal Years 1999–2010*, Report No. FAA APO-99-1, Federal Aviation Administration, Office of Aviation Policy and Plans, Statistics and Forecast Branch, Washington, D.C., March 1999.
- [14] Federal Aviation Administration, *Airport Capacity Enhancement Plan*, 800 Independence Avenue, SW, Washington, D.C., 1998.
- [15] Bureau of Transportation Statistics, *The 1995 American Travel Survey*, 400 7th Street, S.W., Suite 3430, Washington, D.C., 20590.
- [16] American Airlines, *Free Flight: Preserving Airline Opportunity*, Captain Russell G. Chew, September 1997.
- [17] Boeing, *2000 Current Market Outlook*, Boeing Commercial Airplane Group Marketing, P.O. Box 3707, Seattle, WA 98124–2207.
- [18] Salah G. Hamzawi, “Lack of Airport Capacity: Exploration of Alternative Solutions,” *Transportation Research*, Vol. 26A, No.1, 1992, pp. 47–58.
- [19] Moshe Ben-Akiva, and Steven R. Lerman, *Discrete Choice Analysis: Theory and Application to Travel Demand*, The MIT Press, Cambridge, Massachusetts, 1985.
- [20] Kenneth J. Button, *Transport Economics*, 2nd Edition, Edward Elgar Publishing Company, Brookfield, Vermont, 1992.
- [21] Kenneth Train, *Theory, Econometrics, and an Application to Automobile Demand*, The MIT Press, Cambridge, MA, 1986.
- [22] Kenneth Train, “The Potential Market for Non-Gasoline-Powered Automobile,” *Transportation Research*, Vol. 14A, 1980, pp. 405–414.
- [23] Steven D. Beggs, and N. Scott Cardell, “Choice of Smallest Car by Multi-Vehicle Households and the Demand for Electric Vehicles,” *Transportation Research*, Vol. 14A, 1980, pp. 389–404.
- [24] Adib Kanafani, *Transportation Demand Analysis*, McGraw-Hill, New York, 1983.

- [25] Kingsley E. Haynes and A. Stewart Fotheringham, *Gravity and Spatial Interaction Models*, Sage Publications, Beverly Hills, California, 1985.
- [26] Mokhtar S. Bazaraa and C.M. Shetty, *Nonlinear Programming*, John Wiley & Sons, New York, 1979.

Appendix A

Parameter Estimation of the Gravity Model

To use the gravity model to derive the O&D traffic t_{ij} , $i, j = 1, 2, \dots, N$, we must first calibrate the model to get the parameters a_i, b_i , $i = 1, 2, \dots, N$, which are based on the conservation equation, Equation 3-3. If the coupling parameter c_{ij} is determined by the distance between two airports as given by Equation 3-6, then

$$c_{ij} = c_{ji}, \quad i, j = 1, 2, \dots, N \quad [\text{Eq. A-1}]$$

$$c_{ij} \geq 0, \quad i, j = 1, 2, \dots, N, \quad [\text{Eq. A-2}]$$

$$c_{ii} = 0, \quad i = 1, 2, \dots, N. \quad [\text{Eq. A-3}]$$

since $d_{ij} = d_{ji}$, and $f(\cdot) \geq 0$ and $f(0) = 0$ by our assumption. If the coupling parameters c_{ij} , $i, j = 1, 2, \dots, N$, are symmetric, then

$$a_i = b_i, \quad i = 1, 2, \dots, N. \quad [\text{Eq. A-4}]$$

Thus, the gravity model can be restated as

$$t_{ij} = c_{ij} \cdot a_i \cdot T_i \cdot a_j \cdot T_j, \quad i, j = 1, 2, \dots, N, \quad [\text{Eq. A-5}]$$

satisfying

$$\sum_j c_{ij} \cdot a_i \cdot T_i \cdot a_j \cdot T_j = T_i, \quad i = 1, 2, \dots, N. \quad [\text{Eq. A-6}]$$

If we assume uniformity, i.e.,

$$a_i = a_j = a, \quad i, j = 1, 2, \dots, N, \quad [\text{Eq. A-7}]$$

then by summing all the equations for $i=1$ through N , we get

$$a^2 \sum_{i,j} c_{ij} T_i \cdot T_j = \sum_i T_i \quad [\text{Eq. A-8}]$$

or

$$a = \sqrt{\frac{\sum_i T_i}{\sum_{i,j} c_{ij} T_i \cdot T_j}} \quad [\text{Eq. A-9}]$$

Although this is a popular method to estimate the parameters, it does not yield satisfactory calibration. However, it does serve as a starting point for other methods based on iteration.

Let

$$x_i = a_i \cdot T_i \geq 0, \quad i = 1, 2, \dots, N, \quad [\text{Eq. A-10}]$$

then the calibration function of the gravity model is

$$x_i \sum_j c_{ij} \cdot x_j = T_i, \quad i = 1, 2, \dots, N. \quad [\text{Eq. A-11}]$$

By rearranging Equation A-11, we get

$$x_i = \frac{T_i}{\sum_j c_{ij} \cdot x_j}, \quad i = 1, 2, \dots, N. \quad [\text{Eq. A-12}]$$

This is a direct substitution method to solve the nonlinear equation, i.e.,

$$x_i^{(k+1)} = \frac{T_i}{\sum_j c_{ij} \cdot x_j^{(k)}}, \quad i = 1, 2, \dots, N, \quad [\text{Eq. A-13}]$$

where $x_i^{(k)}$ is the k th iteration of x_i . Although simple and straightforward, this method does not yield a convergent solution because it is not a contraction mapping (proof omitted).

Let

$$F_i = x_i \sum_j c_{ij} \cdot x_j - T_i = 0, \quad i = 1, 2, \dots, N, \quad [\text{Eq. A-14}]$$

and $\underline{F} = (F_1, F_2, \dots, F_N)'$. The Newton-Ralphson method, a popular way to find the roots of nonlinear Equation A-11, is given by

$$x_i^{(k+1)} = x_i^{(k)} + \delta x_i^{(k)}, \quad i = 1, 2, \dots, N, \quad [\text{Eq. A-15}]$$

where $\underline{\delta x} = (\delta x_1, \delta x_2, \dots, \delta x_N)'$ is the solution of the linear equation

$$J \cdot \delta x = -F. \quad [\text{Eq. A-16}]$$

J is the Jacobian matrix of \underline{F} , defined as

$$J_{ij} = \frac{\partial F_i}{\partial x_j}, \quad i, j = 1, 2, \dots, N. \quad [\text{Eq. A-17}]$$

Substituting Equation A-11 for Equation A-17 yields

$$J_{ij} = x_i \cdot c_{ij}, \quad i, j = 1, 2, \dots, N. \quad [\text{Eq. A-18}]$$

If Equation A-17 is substituted in Equation A-16, we get

$$x_i^{(k)} \sum_j c_{ij} \cdot \delta x_j^{(k)} = -x_i^{(k)} \sum_j c_{ij} \cdot x_j^{(k)} + T_i, \quad i = 1, 2, \dots, N, \quad [\text{Eq. A-19}]$$

or

$$x_i^{(k)} \sum_j c_{ij} (x_j^{(k)} + \delta x_j^{(k)}) = T_i, \quad i = 1, 2, \dots, N, \quad [\text{Eq. A-20}]$$

or

$$x_i^{(k)} \sum_j c_{ij} \cdot x_j^{(k+1)} = T_i, \quad i = 1, 2, \dots, N. \quad [\text{Eq. A-21}]$$

In terms of matrices,

$$C \cdot x^{(k+1)} = d^{(k)}, \quad [\text{Eq. A-22}]$$

where $\underline{d}^{(k)} = (d_1, d_2, \dots, d_N)^t$, and

$$d_i = \frac{T_i}{x_i}, \quad i = 1, 2, \dots, N. \quad [\text{Eq. A-23}]$$

Then,

$$x^{(k+1)} = C^{-1} \cdot d^{(k)}. \quad [\text{Eq. A-24}]$$

In theory, if we can carry the iteration forward, eventually we will get the convergence and solve the nonlinear equation. In practice, this iteration scheme does not work because it requires taking the inverse of a large dimension matrix (2,865×2,865). It is impractical even if we solve the linear equation Equation A-21 directly through the LU decomposition because it requires many iterations to solve the nonlinear equations. We must seek another solution.

It is not necessary to force the conservation equation, Equation A-6, strictly in calibrating the gravity model because our GA network, although comprehensive, still leaves about 8 percent of GA traffic uncovered. Undoubtedly this traffic will come to our GA network airports. Understanding this, we can restate the gravity calibration problem as a nonlinear programming problem:

$$\min : f(x) = \sum_i s_i^2 \quad [\text{Eq. A-25}]$$

$$\text{subject to: } x_i \sum_j c_{ij} \cdot x_j - s_i = T_i, \quad i = 1, 2, \dots, N, \quad [\text{Eq. A-26}]$$

and

$$x_i \geq 0, \quad i = 1, 2, \dots, N.$$

\underline{s} is a vector of slack variables. Obviously, when $\underline{s} = \underline{0}$, we get the exact solution for the gravity calibration. In practice, we need only to minimize the objective function $f(\underline{x})$ until the convergence is found. For this report, we used the following criterion:

$$\max \left\{ \left| \frac{s_i}{T_i} \right| \right\} < \varepsilon \quad [\text{Eq. A-27}]$$

and we select ε to be 0.05, well within the range of 8 percent implied by the data.

We used the deepest decent method to solve the nonlinear programming [26]. The iteration is carried by the following:

$$\underline{x}^{(k+1)} = \underline{x}^{(k)} - h \nabla \left(f(\underline{x}^{(k)}) \right) \quad [\text{Eq. A-28}]$$

where $\nabla(\cdot)$ is the gradient of the objective function $f(\cdot)$ and h represent the scalar step size. The optimal step size can be determined using the following formula:

$$h = \frac{\nabla f(\underline{x}^{(k)})^t \cdot \nabla f(\underline{x}^{(k)})}{\nabla f(\underline{x}^{(k)})^t H(\underline{x}^{(k)}) \nabla f(\underline{x}^{(k)})}. \quad [\text{Eq. A-29}]$$

By definition,

$$\nabla f(\underline{x}) = \left[\frac{\partial f(\underline{x})}{\partial f(x_i)} \right]^t \quad [\text{Eq. A-30}]$$

and from Equation A-25,

$$\frac{\partial f(\underline{x})}{\partial f(x_k)} = 2 \sum_i s_i \frac{\partial s_i}{\partial x_k}. \quad [\text{Eq. A-31}]$$

By Equation A-26,

$$\frac{\partial s_i}{\partial x_k} = \frac{\partial}{\partial x_k} \left(x_i \sum_j c_{ij} x_j - T_i \right) = \begin{cases} x_i \cdot c_{ik}, & k \neq i \\ \sum_j c_{kj} \cdot x_j, & k = i \end{cases} \quad [\text{Eq. A-32}]$$

If we substitute Equation A-32 into Equation A-31, we get

$$\begin{aligned} \frac{\partial f(x)}{\partial x_k} &= 2 \left(s_k \sum_j c_{kj} \cdot x_j + \sum_i s_i \cdot x_i \cdot c_{ik} \right) \\ &= 2 \left(\sum_j c_{jk} \cdot s_k \cdot x_j + \sum_i c_{ik} \cdot s_i \cdot x_i \right) \\ &= 2 \sum_i c_{ik} (s_i + s_k) x_i. \end{aligned} \quad [\text{Eq. A-33}]$$

The Hessian matrix $\mathbf{H} = (H_{ij})$ is defined as the second derivative of the objective function f . By Equation A-33,

$$\frac{1}{2} H_{kl} = \frac{1}{2} \frac{\partial^2 f}{\partial x_k \partial x_l} = H1 + H2 + H3, \quad [\text{Eq. A-34}]$$

where

$$\begin{aligned} H1 &= \sum_i c_{ki} \frac{\partial s_i}{\partial x_l} x_i \\ &= c_{kl} \sum_j c_{lj} x_j + \sum_i c_{ki} \cdot c_{li} \cdot x_i \\ &= \sum_i c_{kl} \cdot c_{li} \cdot x_i + \sum_i c_{ki} \cdot c_{li} \cdot x_i \\ &= \sum_i c_{li} (c_{ki} + c_{kl}) x_i. \end{aligned} \quad [\text{Eq. A-35}]$$

$$H2 = \begin{cases} c_{kl} \cdot x_k \cdot \sum_i c_{ki}, & l \neq k, \\ \sum_i c_{ki} \left(\sum_j c_{lj} \cdot x_j \right), & l = k. \end{cases} \quad [\text{Eq. A-36}]$$

$$H3 = c_{kl} (s_k + s_l). \quad [\text{Eq. A-37}]$$

After we know the gradient vector and the Hessian matrix, we can carry out iteration according to the deepest decent algorithm.

There is excessive computation in computing the optimal step size. It is faster to use a fixed step size, which is determined by trial and error. We found 4.0×10^{-6} is the largest step size without jeopardizing the convergence of solution.

REPORT DOCUMENTATION PAGE			Form Approved OMB No. 0704-0188	
Public reporting burden for this collection of information is estimated to average 1 hour per response, including the time for reviewing instructions, searching existing data sources, gathering and maintaining the data needed, and completing and reviewing the collection of information. Send comments regarding this burden estimate or any other aspect of this collection of information, including suggestions for reducing this burden, to Washington Headquarters Services, Directorate for Information Operations and Reports, 1215 Jefferson Davis Highway, Suite 1204, Arlington, VA 22202-4302, and to the Office of Management and Budget, Paperwork Reduction Project (0704-0188), Washington, DC 20503.				
1. AGENCY USE ONLY (Leave blank)		2. REPORT DATE June 2001	3. REPORT TYPE AND DATES COVERED Contractor Report	
4. TITLE AND SUBTITLE A Small Aircraft Transportation System (SATS) Demand Model			5. FUNDING NUMBERS C NAS2-14361 WU 522-99-11-01	
6. AUTHOR(S) Dou Long, David Lee, Jesse Johnson, and Peter Kostiuk				
7. PERFORMING ORGANIZATION NAME(S) AND ADDRESS(ES) Logistics Management Institute 2000 Corporate Ridge McLean, Virginia 22102-7805			8. PERFORMING ORGANIZATION REPORT NUMBER LMI-NS004S1	
9. SPONSORING/MONITORING AGENCY NAME(S) AND ADDRESS(ES) National Aeronautics and Space Administration Langley Research Center Hampton, VA 23681-2199			10. SPONSORING/MONITORING AGENCY REPORT NUMBER NASA/CR-2001-210874	
11. SUPPLEMENTARY NOTES Langley Technical Monitor: Robert Yackovetsky Final Report				
12a. DISTRIBUTION/AVAILABILITY STATEMENT Unclassified-Unlimited Subject Category 05 Distribution: Nonstandard Availability: NASA CASI (301) 621-0390			12b. DISTRIBUTION CODE	
13. ABSTRACT (Maximum 200 words) The Small Aircraft Transportation System (SATS) demand modeling is a tool that will be useful for decisionmakers to analyze SATS demands in both airport and airspace. We constructed a series of models following the general top-down, modular principles in systems engineering. There are three principal models, SATS Airport Demand Model (SATS-ADM), SATS Flight Demand Model (SATS-FDM), and LMINET-SATS. SATS-ADM models SATS operations, by aircraft type, from the forecasts in fleet, configuration and performance, utilization, and traffic mixture. Given the SATS airport operations such as the ones generated by SATS-ADM, SATS-FDM constructs the SATS origin and destination (O&D) traffic flow based on the solution of the gravity model, from which it then generates SATS flights using the Monte Carlo simulation based on the departure time-of-day profile. LMINET-SATS, an extension of LMINET, models SATS demands at airspace and airport by all aircraft operations in U.S. The models use parameters to provide the user with flexibility and ease of use to generate SATS demand for different scenarios. Several case studies are included to illustrate the use of the models, which are useful to identify the need for a new air traffic management system to cope with SATS.				
14. SUBJECT TERMS Small Aircraft Transportation System, SATS, LMINET, LMINET-SATS, air transportation demand model, gravity model			15. NUMBER OF PAGES 77	
			16. PRICE CODE	
17. SECURITY CLASSIFICATION OF REPORT Unclassified	18. SECURITY CLASSIFICATION OF THIS PAGE Unclassified	19. SECURITY CLASSIFICATION OF ABSTRACT Unclassified	20. LIMITATION OF ABSTRACT UL	